Self-extinguishing and hydrophobic epoxy composites containing hydrothermal liquefaction-derived biochar and whisker-like particles based on tailored PVP-coated silica

Self-extinguishing and hydrophobic epoxy composites containing hydrothermal liquefaction-derived biochar and whisker-like particles based on tailored PVP-coated silica fibers

Immacolata Mazzuoccolo[a,#], Immacolata Climaco[a,#], Jessica Passaro[b], Francesca Di Lauro[a,f], Daniele Battegazzore[d], Milijana Jovic[e], Pietro Russo[b], Giulio Malucelli[d], Sabyasachi Gaan[e], Antonio Aronne[a], Fabio Montagnaro[c,f], Marco Balsamo[c], Claudio Imparato[a,*], Aurelio Bifulco[a,*]

[a]Department of Chemical, Materials and Production Engineering, University of Naples Federico II, 80125 Naples, Italy

[b]Institute for Polymers, Composites and Biomaterials, National Council of Research, 80078 Pozzuoli, Italy

[c]Department of Chemical Sciences, University of Naples Federico II, Complesso Universitario di Monte Sant'Angelo, 80126 Naples, Italy

[d]Department of Applied Science and Technology, Politecnico di Torino, 15121 Alessandria, Italy

[e]Advanced Fibers Laboratory, Swiss Federal Laboratories for Materials Science and Technology (Empa), 9014 St. Gallen, Switzerland

[f]Institute of Sciences and Technologies for Sustainable Energy and Mobility, National Research Council, 80125 Naples, Italy

* Corresponding authors: claudio.imparato@unina.it (C.I.); aurelio.bifulco@unina.it (A.B.)

[#] I.M. and I.C. contributed equally to this work.

Abstract

The hydrothermal liquefaction (HTL) of waste biomass produces bio-oil along with solid, aqueous, and gaseous co-products. The utilization of solid residue (biochar) is a crucial step in achieving the sustainability and circularity of the entire HTL process. Here, we propose the valorization of biochar derived from HTL of municipal sewage sludge as a functional additive for epoxy resins to enhance their flame retardancy. Biochar samples from HTL, obtained under different operative conditions, were characterized and incorporated into an epoxy resin cured with a cycloaliphatic amine. Biochar was used in combination with whisker-like particles, made of silica coated with electrospun poly(vinylpyrrolidone) (PVP) and functionalized to enhance compatibility with the polymer matrix. The synergy of these fillers with ammonium polyphosphate and urea enabled the preparation of no-drip self-extinguishing composites (V0 rating at UL-94 vertical flame spread tests), showing excellent fire performance, as assessed by cone calorimetry and pyrolysis combustion flow calorimetry, with a limited effect on the viscoelastic behavior and some impact on the flexural properties. Notably, a strong flame retardant action in the condensed phase, with a slight effect in the gas phase, was responsible for the formation of a ceramic continuous char, which decreased the peak of the heat release rate (~36%) as well as the total smoke release (~10%) during the burning process. Besides, the tailored whisker-like particles were able to migrate at the surface of composites, providing water contact angles of ~120°, suggesting a potential use of the designed materials as water-proof protective coatings or components for multifunctional infrastructures.

Keywords: Epoxy resin, municipal sewage sludge, hydrothermal liquefaction, biochar, flame retardancy, combustion behaviour.

Highlights

- Biochar from hydrothermal liquefaction was valorized as filler in epoxy systems.
- Biochar enabled the reduction of total smoke release (~10%) and peak heat release rate (~36%).
- Functionalized silica-based whisker-like microparticles were incorporated in the epoxy.
- The composites containing 10 wt.% of biochar and 1 wt.% of P loading achieved self-extinction.
- The composites showed hydrophobic surface and a limited mechanical response.

1. Introduction

In recent years, human activities have been responsible for growing environmental impacts in terms of depletion of natural resources and increased waste production [1]. Hence, a transition from a linear economic model toward a more sustainable circular approach, considering waste as a resource in the design of new products, opens opportunities for technological development [2] supported by governmental policies, such as the European Next Generation EU program [3]. In the manufacturing of polymer-based products, the use of additives is crucial to fulfill functional and mechanical performance requirements. However, such compounds mostly derive from nonrenewable sources and can pose ecological concerns in the use and recycling of polymeric materials, mainly due to the release of toxic species [4,5]. Among thermosetting polymers, epoxy resins are used to develop a large array of high-performance products, including laminates, panels, adhesive layers, tubes/pipes, which must usually comply with severe fire safety standards and regulations [6,7]. Polymeric coatings, often based on epoxy resins, with high adhesion and chemical resistance toward salts and solvents, can ensure protection against water (or water vapor) to building materials, like concrete or wood. Such coatings, employed for roofing, flooring, and waterproofing of tanks and pipes, are typically subject to fire testing (e.g., EU: ENV 1187:2002; US: ASTM E648, E84) [8], and thus require flame retardant additives [9].

In this field, it is crucial to replace harmful halogen-based flame retardants. Phosphorus- and nitrogen-containing additives (e.g., ammonium polyphosphate (APP), phytic acid, urea, and melamine), inorganic particles (e.g., silica, metal hydroxides), and biomass-derived materials (e.g., chitosan, lignin, spent coffee grounds) have been investigated as greener alternatives [10,11]. Recently, nano/micro-structures prepared from electrospun fibers have revealed their potential in the manufacturing of polymeric materials with improved fire behavior, due to their specific morphology, superior active surfaces, and low-cost synthesis [12,13]. For instance, nanofibers based on poly(vinylpyrrolidone) (PVP), a biocompatible polymer, easily obtained by electrospinning for biomedical or environmental systems [14,15], can incorporate silica nanoparticles and undergo thermal treatment to counter their water solubility and flammability [16–18]. Thus, materials derived from silica-filled fibers could be interesting candidates in the scope of flame retardancy.

Turning to biomass-derived and biowaste materials, their use as renewable components of polymer-based systems represents a promising approach toward improved sustainability and circularity [19,20]. On the other hand, sizeable amount of these compounds must often be incorporated into the epoxy matrix to achieve satisfying fire performances. As an example, Vahabi et al. modified spent coffee grounds with dimethyl phosphite to obtain a functional filler for a bisphenol A diglycidyl ether (DGEBA) resin, finding that 30 wt.% of this additive was needed to lower the flammability and

reduce the peak of heat release rate by 40%, compared to the virgin sample [21]. In this context, growing attention is raised by biochar, the solid product resulting from the thermochemical conversion of biomasses (e.g., wastes deriving from agriculture and food industry or municipal sludge) [19]. Biochar has great significance for carbon sequestration, contributing to carbon neutrality and greenhouse effect mitigation, and has been applied as a soil conditioner to reduce the need for fertilizers and pesticides in agricultural production [22–24]. It can also be employed as an additive for plastics and molding materials, owing to its highly carbon-enriched skeleton, porous supramolecular surface structure, and oxygen-containing functional groups [25]. The effect of the addition of biochar particles with different morphologies on the mechanical and electrical properties of epoxy resin was extensively studied by Bartoli, Giorcelli, and coworkers [26–28]. The composition and architecture of biochar allow it to establish good physical interactions with the polymer matrix, and to promote the charring process and the formation of an effective thermal shield during the polymer degradation upon exposure to heat or fire [29,30]. Particularly, the combined use of APP and biochar has been found to significantly enhance the flame retardant performance of polymers, offering a sustainable and cost-effective solution in reducing fire risks [31,32]. This is due to the intumescent and char-promoting properties of APP, joint with the ability of biochar in forming a robust char layer, strengthening the thermal stability of the residue. Their synergistic action also slows down fire propagation and helps reduce the flammability and smoke production of polymeric composites [33,34]. Recently, the introduction of 20 wt.% biochar into a modified epoxy matrix along with a Si-Ti-Mg mixed oxide and APP allowed to obtain thermally stable self-extinguishing composites, with a strongly reduced heat release rate and a decrease (∼11%) in the total smoke production [33].

Notwithstanding these promising results, the exploitation of biochar as a flame retardant has been poorly investigated to date. Other examples include the incorporation of 30 wt.% biochar and 40 wt.% $Mg(OH)_2$ into high-density polyethylene, which increased the limiting oxygen index (LOI) from 23.9% to 31.9% while keeping good flexural strength [25], and the preparation of an all-bio-sourced waterborne system comprising phytic acid and biochar to improve the fire behavior of cotton fabrics, providing self-extinction in UL-94 flame spread tests with a limited dry add-on (8 wt.%) [35].

When planning the use of biochar as an additive, it should be considered that its chemical and structural features vary widely according to the starting material and the production process. Biochar is a typical co-product of hydrothermal liquefaction (HTL), a thermochemical depolymerization process carried out to convert wet biomass into biocrude oil as target product and other chemicals at moderate temperature (typically 200–400 °C) and high pressure (10–25 MPa) [22,36], avoiding the energy-intensive drying step associated to conventional combustion and gasification. The HTL of

civil and industrial sludges, generated during wastewater purification treatments, produces a solid biochar, water soluble compounds, and non-condensable gas, in addition to the target biocrude [37]. The average yield of solid residue from HTL processes is around 45%, depending on the feedstock: hence, its valorization is an important goal to improve the sustainability and circularity of this technology [38]. Compared to biochar produced by high-temperature pyrolysis, the one derived from HTL generally shows structural differences [39]: the latter tends to have more abundant oxygen-containing functional groups [40], which make its organic fraction similar to humic acids obtained by the biological and chemical degradation of vegetable and animal biomasses [41,42], and a larger inorganic content. The oxygenated species and the inorganic fraction may increase surface acidity, favouring the dehydration of polymer matrix, and contribute to a flame retardant action in the condensed phase, resulting in a robust final carbonaceous residue. Despite these suitable features of HTL biochar, its potential in improving the thermal and fire behavior of thermosets is still unexplored. The HTL of different sludges for the production of bio-oil is being actively investigated [43–45]. With the aim of developing an integrated biorefinery process with optimized exploitation of mass and energy and minimized waste generation, we are proposing the reuse of the resulting biochar as filler in epoxy-based materials. In this work, we report a comprehensive characterization of the composites obtained by incorporating biochar into an epoxy resin, also combined with whisker-like particles derived from electrospun PVP-silica fibers and widely available flame retardants (urea and APP). The optimal composition provided very low flammability (V0 rating in UL-94 flame spread tests), neatly enhanced fire performances, measured by cone calorimetry, and good thermal resistance, with a limited impact on mechanical behavior.

This study represents the first report on the valorization of biochar from HTL as functional additive in a polymeric material. The results reveal how the characteristics of different biochar samples influence their effect and how the synergy with other additives boosts the properties of the final composites. This approach appears as a viable waste reutilization pathway, conferring added value to the residue of a waste transformation process.

2. Materials and methods

2.1. Materials

The biochar used in this study derives from the hydrothermal liquefaction process of municipal sewage sludge deriving from a wastewater treatment plant located in Milan (Italy), tested in a previous experimental campaign [43–45]. Previous proximate and ultimate analysis indicated that the sludge has moisture, volatile matter, fixed carbon and ash contents of 12.1, 57.4%, 21.1% and 9.3%,

respectively, and the elemental composition on a dry basis is 34.6% (C), 4.9% (H), 5.9% (N), and 0.8% (S).

Poly(vinylpyrrolidone) (PVP, 1,300,000 g mol^{-1}) and tetraethyl orthosilicate (TEOS, 98%), purchased from Sigma-Aldrich (St. Louis, USA), were the starting materials for the synthesis of PVP-silica fiber blankets, which will be named PVP-Si. Their functionalization was performed using (3-glycidyloxypropyl)trimethoxysilane (GPTMS, 98%) as a coupling agent, purchased from Sigma-Aldrich (St. Louis, USA), and isophorone diamine (IPDA), a cycloaliphatic diamine hardener, provided by Mates S.r.l. (Milan, Italy). The composite materials were prepared employing an epoxy system (SX10) from Mates S.r.l. (Milan, Italy), composed of Bisphenol A diglycidyl ether (DGEBA) and IPDA. Urea and ammonium polyphosphate (APP), acquired from Sigma-Aldrich (St. Louis, USA), were used as flame retardant additives.

2.2. Production of biochar by hydrothermal liquefaction

A detailed description of the experimental apparatus and protocol used for biochar production is reported in [43]. Briefly, it consists in a 500 mL Hastelloy C-276 batch stirred reactor (Parr Instruments, series PA 4575A) equipped with a digital pressure transducer coupled with a needle valve for pressure measurement and control, and a heating system combining cylindrical blocks and a band heater. HTL experimental tests were carried out at 200 bar for slurries containing 10 wt.% sludge in the aqueous phase. The HTL operating conditions for the production of biochar were the ones that in a previous work determined the best yield of the target biocrude: set point temperatures of 300 °C and 350 °C, with isothermal holding times of 10 min and 30 min at each temperature [43]. After the HTL test, the liquid and solid phases were recovered from the vessel with a spatula, and 30 g of dichloromethane (DCM) were added to maximise the products recovery. The resulting slurry was filtered on a Büchner under vacuum. After filtration, focusing on biochar recovery, the solid phase was subjected to Soxhlet extraction to recover the biocrude from the solid pores, using about 150 g of DCM as extracting solvent. At the end of this operation, the solid residue was oven-dried at 105 °C for 24 h. The biochar samples were named Ch_X-Y, where X is the set temperature for the isothermal stage (300 or 350 °C) and Y is the isothermal time at the set temperature (10 or 30 min).

2.3. Preparation of functionalized PVP-silica particles

PVP-Si blankets were fabricated using the electrospinning technique. The procedure was reported in a previous publication, and the main steps are briefly mentioned in the following [18]. Sol–gel method was employed to prepare SiO_2 nanoparticles starting from TEOS as a precursor. PVP was dispersed in an ethanol solution (20 wt.%) and mixed with a suspension (40 wt.%) of silica particles in ethanol.

The mixture was electrospun under a voltage of 30 kV by keeping the room temperature and humidity of (45 ± 10)% and ensuring a flow rate of 0.100 mL/min. The electrospun non-woven mats were dried at 80 °C for 60 min, then heat-treated from 150 to 200 °C, and finally maintained at 200 °C for 6 h to cross-link the fibers. The thermal treatment of PVP-Si blankets gives them resistance to humidity, while the sol-gel particles embedded into the fibers become exposed at the surface and able to be functionalized [18,46].

The PVP-Si fibers were further treated to enhance their compatibility with the epoxy resin and to make them easily dispersible in the polymer matrix. The procedure is schematized in Figure 1. A solution containing 10 v/v% GPTMS in a 20/80 v/v% water/ethanol mixture was added dropwise using a micropipette onto PVP-Si fragments (4 mL/1 g); the impregnated fibers were dried at 80 °C for 30 min in a ventilated oven, giving G-PVP-Si samples. Then, a 0.4 g/mL IPDA solution in acetone was added dropwise onto dried G-PVP-Si fibers, as described above. After drying at 80 °C for 12 h, a functionalized material, referred to as GI-PVP-Si, was obtained. GI-PVP-Si was finally ground in an agate mortar and by ball milling, with a Mixer Mill MM 400 (Retsch, Haan, Germany) for 2 min at 25 Hz, resulting in a fine powder. The morphology of initial PVP-Si fiber mats and GI-PVP-Si powders is shown in Figure 1.

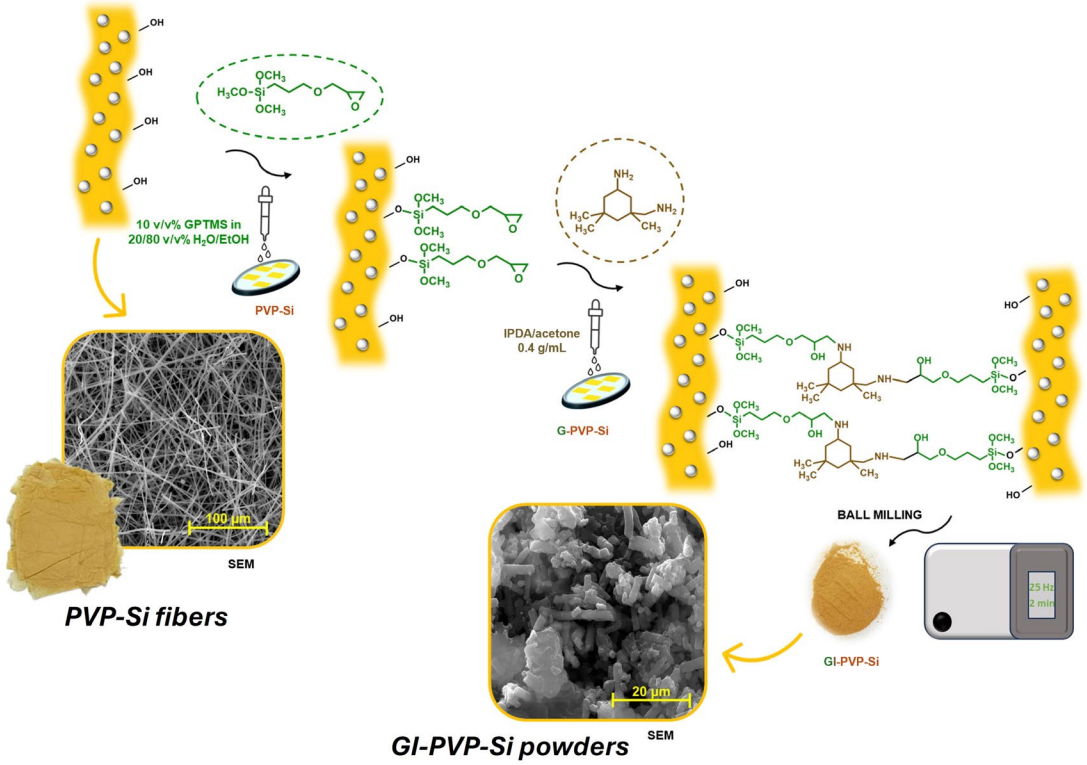

Figure 1. Scheme of the preparation procedure of functionalized PVP-Si particles. Photographs and SEM images of PVP-Si fibers and GI-PVP-Si powders are also shown.

2.4. Preparation of epoxy composites

In a typical procedure, the selected biochar (see section 3.1), urea, APP, and GI-PVP-Si (see Table 1 and section 2.3) were mixed and ground in a mortar. The powder mixture was dried at 80 °C for 30 min and then incorporated into DGEBA resin. The system was stirred using a vortex to obtain a uniform distribution of the additives in the polymer matrix. Finally, IPDA (26 wt.% with respect to the DGEBA resin) was added into the system to start the curing process (60 °C/12 h and 80 °C/4 h) in a silicone rubber mold. The whole synthesis procedure of epoxy composites is displayed in Figure 2, while the composition of all the prepared samples is listed in Table S1. In particular, the composition of the fully characterized epoxy systems is reported in Table 1.

To give an example of the meaning of the samples' codes, ECUA5PS1P represents the epoxy (E) formulation containing the biochar (C, 10 wt.%), urea (U, 2 wt.%), APP (A, 3 wt.%), GI-PVP-Si (PS, 5 wt.%), and 1 wt.% of P as APP, considering the nominal content of P in APP as ~30 wt.% (Table 1 and Table S1).

Table 1. Composition of the fully characterized epoxy-based samples. The mass percentages are referred to (DGEBA+IPDA) basis.

Sample	DGEBA (wt.%)	IPDA (wt.%)	Ch_300-30 (wt.%)	APP (wt.%)	UREA (wt.%)	GI-PVP-Si (wt.%)	P[a] (wt.%)
E	79.4	20.6	-	-	-	-	-
EC	79.4	20.6	10	-	-	-	-
E5PS	79.4	20.6	-	-	-	5	-
EC5PS	79.4	20.6	10	-	-	5	-
ECUA5PS1P	79.4	20.6	10	3	2	5	1

[a] nominal content of phosphorus

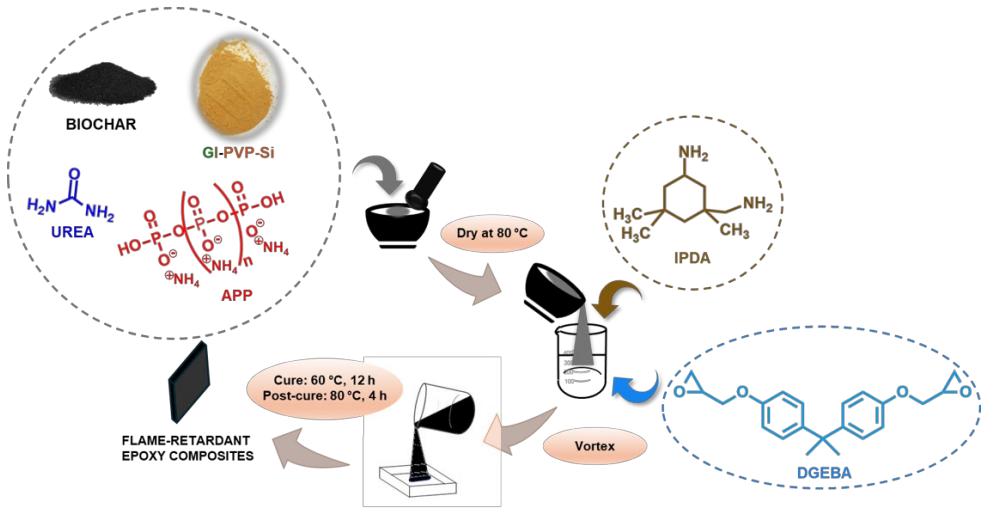

Figure 2. Synthesis procedure of epoxy composites.

2.5. Characterization techniques

240 The chemical composition of the four biochar samples produced by HTL was investigated by Fourier
241 Transform InfraRed spectroscopy, ultimate and proximate analysis.
242 **Fourier Transform InfraRed (FTIR)** spectra were collected using a Nicolet 5700
243 (Thermoscientific, Waltham, MA, USA) with a DTGS KBr detector in the range from 400 to 4000
244 cm^{-1}. The IR transmittance spectra of powders mixed in KBr pellets were collected as the sum of 32
245 scans with a resolution of 2 cm^{-1}.
246 **Proximate analysis** was carried out by reference to UNI 9903/ASTM D5142 standards and using a
247 TGA701 LECO thermobalance to evaluate moisture, volatile matter, fixed carbon and ash in the
248 biochar.
249 **Ultimate analysis** was obtained by means of a LECO CHN628 analyzer and according to ASTM
250 reference standard D5373 to determine C, H, and N contents in the biochar; the S percentage in the
251 solid samples was evaluated via an elementary LECO SC-144DR analyzer and using as reference
252 standard the UNI 7584.
253 Ch_300-30 was also investigated by **scanning electron microscopy (SEM)** equipped with an
254 **energy-dispersive X-ray (EDX)** detector (FEI Quanta 200 FEG SEM equipped with an Oxford Inca
255 Energy System 250 and an Inca-X-act LN2-free analytical silicon drift detector). SEM investigations
256 were performed using a FEI Quanta 200 FEG SEM (Thermo Fisher Scientific Inc., USA) operating
257 in high vacuum conditions (~10^{-5} mbar). The measurements were conducted using a secondary
258 electron detector, applying an accelerating voltage from 10 to 30 kV.
259 PVP-Si and GI-PVP-Si were analysed by FTIR spectroscopy and SEM-EDX analysis, using the
260 abovementioned instruments.
261 The wettability of pure resin and epoxy composites was evaluated using a Dataphysics OCA 30
262 instrument. **Water contact angle (WCA)** measurements were performed at ~25 °C, placing water
263 droplets with a volume of 6-9 μL on the surface of thermosetting substrates [47].
264 The epoxy-based composites were analysed by FTIR spectroscopy, and their thermal properties were
265 assessed by **differential scanning calorimetry (DSC)** and **thermogravimetric analysis (TGA)**.
266 DSC measurements were carried out using a Mettler DSC 822/400 thermal analyzer (Mettler-Toledo,
267 Columbus, OH, USA), applying a typical procedure consisting of three consecutive heating-cooling-
268 heating stages, over the temperature range between 20 °C and 300 °C, with a thermal scanning rate
269 of 10 °C/min, under a nitrogen atmosphere (flow rate: 50 mL/min). The glass transition temperature
270 was identified at the inflection point of the second heating scan. TGA was carried out on the biochar
271 samples and epoxy composites using a Mettler TGA/SDTA 851 instrument (Mettler-Toledo
272 Columbus, OH, USA) under air and N_2 atmospheres with a flow rate of 50 mL/min for both. Weight

loss profiles were recorded as a function of temperature by heating the samples from 25 °C to 800 °C at 10 °C/min.

The viscoelastic behavior of the materials was assessed through **dynamic mechanical analysis (DMA)** carried out using a DMA 850 (TA Instrument, USA) operating in dual cantilever mode to evaluate the storage (E′), loss moduli, and tanδ vs. temperature of pristine resin and epoxy nanocomposites. All samples (60 × 10 × 3 mm^3) were characterized through a heating ramp from -30 °C to 180 °C at 2 °C/min. A sinusoidal load was applied at a frequency of 1 Hz with an amplitude of 10 μm. Glass transition temperature was determined as the maximum of the peak of the tanδ curve.

Three-point bending tests were performed, according to ASTM D790, using an Instron 4505 universal testing machine (Instron Corporation, Canton, MA, USA) to evaluate the flexural behaviour. The setup included a 1 kN load cell, a crosshead speed of 2 mm/min, and a span length of 50 mm. The specimens measured 120 × 12 × 3.4 mm^3 and the recorded results were averaged on at least five samples.

The **flammability** of all epoxy composites was assessed by UL-94 vertical flame spread tests (IEC 60695-11-10; sample dimensions: 13 × 125 × 3 mm^3).

Limiting oxygen index (LOI) tests were carried out by using a FIRE oxygen index apparatus according to the ASTM D2863 standard.

To evaluate the fire behavior of pristine resin and epoxy nanocomposites, a **cone calorimeter test** (Noselab ATS, Monza, Italy) was conducted applying an irradiative heat flux of 35 kW/m^2 according to the ISO 5660 standard. Specimens measured 10 × 10 × 0.3 cm^3 and were positioned horizontally on a supporting grid. The cone calorimetry tests were performed to obtain key parameters including the time to ignition (TTI, s), total heat release (THR, MJ/m^2), heat release rate (HRR, kW/m^2), peak of the heat release rate (pHRR, kW/m^2), total smoke release (TSR, m^2/m^2), and specific extinction area (SEA, m^2/kg). Further, in accordance with ASTM D7309 standard, a **pyrolysis combustion flow calorimeter** (**PCFC**, Fire Testing Technology Instrument, London, UK) was employed to evaluate the heat release capacity. The specimens (20-25 mg) were heated from 150 to 750 °C at 1 °C/s in the pyrolysis zone.

3. Results and discussion

3.1. Characterization of biochar samples

The four biochar samples produced by HTL under different conditions were thoroughly characterized in terms of composition, structure, and thermal stability to gain insight into their potential interactions with the polymer matrix and the resulting impact on its behavior. The results of ultimate and proximate analyses, reported in Table S2, indicate that increasing the temperature and time of the

HTL process leads, as expected, to a higher conversion of the organic matrix of the initial sludge. As a result, the content of carbon, hydrogen, nitrogen, and volatiles is reduced in the solid residue, while the ash content increases (Figure 3a). The large ash percentage (ranging from 63 to 80 wt.%) is consistent with the previously reported inductively coupled plasma mass spectrometry (ICP-MS) data, which revealed a considerable concentration of inorganic elements of the starting sludge (especially Fe, P, Ca, Mg, Al) in the solid residues Ch_300-30 and Ch_350-10 [43]. The low moisture content in all biochar samples (1-2 wt.%) makes a drying step before their use unnecessary. Furthermore, with increasing process temperature and isothermal time at 350 °C, a growth in C/H ratio is observed (Table S2), suggesting the presence of larger fractions of cyclic or aromatic compounds, which are more thermally stable than linear chains. The introduction of a carbonaceous filler with high aromatic content into a polymer matrix can positively affect the thermo-oxidative stability of final composites, resulting in a larger amount of residual char after combustion [48,49].

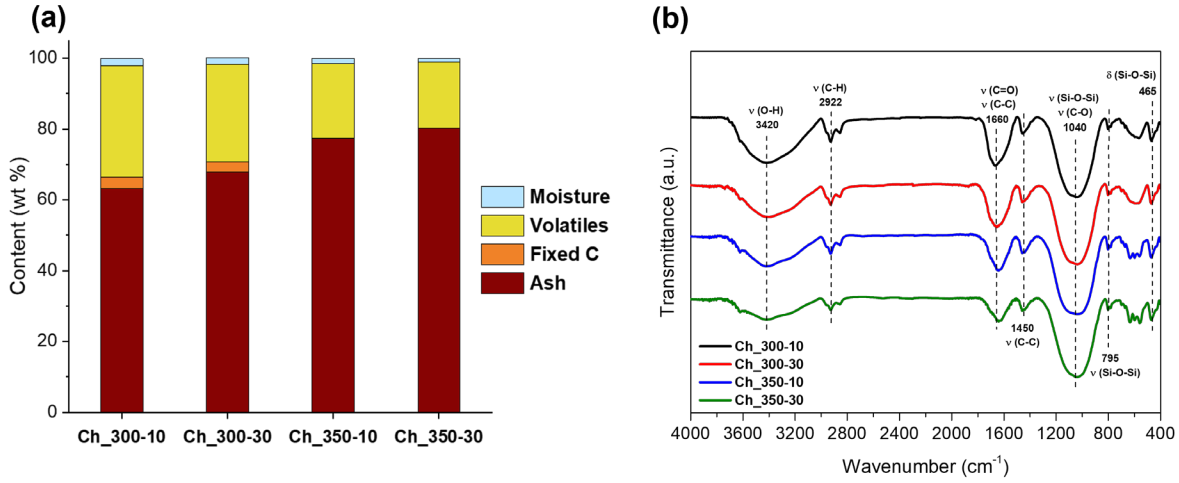

Figure 3. Results of proximate analysis (a) and FTIR spectra (b) of the four biochar samples obtained in different HTL operating conditions.

FTIR spectra (Figure 3b) give further information on the chemical structure of the biochar samples. They display similar profiles, including the broad band associated with O–H bond stretching, centred around 3420 cm^{-1}, aliphatic C–H stretching bands at about 2922 cm^{-1}, a rather wide band around 1660 cm^{-1}, likely due to the overlap of C=O stretching and aryl C–C stretching (seen as a shoulder at about 1600 cm^{-1}), a band commonly assigned to aromatic ring vibrations at 1450 cm^{-1}, a broad and intense band around 1040 cm^{-1}, which could encompass the contribution of Si–O–Si and C–O stretching. The signals at lower wavenumbers can be attributed to other Si–O vibrations, C–H bending in aromatic and unsaturated structures, as well as vibrations of metal–oxygen bonds. Therefore, aliphatic and aromatic units seem to coexist in the organic fraction. The relative intensities of the bands corresponding to the organic groups, along with the O–H stretching one, tend to decrease with

increasing temperature and residence time, in agreement with the observations of ultimate analysis. On the other hand, it can be noted that the shoulder around 3622 cm^{-1}, ascribed to the hydroxyl groups linked to the inorganic component, does not significantly decay with increasing temperature. A structure rich in surface hydroxyl groups may have a partially acidic character and favour the dehydration of the polymer matrix, thus acting as a char promoter.

TGA was performed in both nitrogen and air to evaluate the thermal and thermo-oxidative stability of the biochar samples, respectively (see Figure S1a-d). Figures S1a,b show a larger mass loss for biochar obtained at 300 °C, due to higher volatiles and moisture content (see the proximate analysis data, Table S2). The residues at 800 °C of samples Ch_300-10 and Ch_300-30 are about 10 wt.% lower than those of Ch_350-10 and Ch_350-30, as also shown in Table S3. In oxidative atmosphere (Figure S1b), Ch_350-Y biochars present an almost identical profile to that recorded in pyrolysis, since they contain a lower concentration of volatiles and no fixed carbon. In contrast, Ch_300-Y samples, with a higher carbonaceous content, show a larger mass loss around 350 °C due to the combustion of these components. Overall, the final residues confirm the significant inorganic fraction of HTL biochar, and the differences in the residual mass values recorded in air well agree with the composition variations between the samples.

Ch_300-30 was chosen as the representative biochar for SEM-EDX analysis. Figure S2 shows a SEM micrograph that highlights the rough and apparently porous surface of a Ch_300-30 particle. The surface composition of the sample (Table S4) reveals a carbon percentage approximately double with respect to the value obtained by ultimate analysis, suggesting that the carbonaceous fraction is more concentrated in the outer layers of the biochar particles than in the bulk. After C and O, the most abundant elements detected by EDX in Ch_300-30 are Fe, P, Si, and Ca, in fair accordance with the abovementioned ICP-MS data [43].

The selected HTL biochar, obtained from a process conducted via an isothermal treatment at 350 °C, shows a large fraction of thermally stable compounds with branched or conjugated structures (cyclic or aromatic), whose presence is supported by the high C/H ratio. Aromatic structures are intrinsically more thermally stable due to the resonance stabilization of their delocalized π-electron systems, which require higher energy input to undergo bond scission. Aromatic-rich carbonaceous fillers tend to promote the formation of a thermally stable char layer during heating, which acts as a physical barrier that limits heat flux, mass transport of volatile degradation products, and oxygen diffusion [50,51]. Using HTL biochar as filler may increase the thermal stability of final epoxy composites, also giving a larger amount of residual mass after burning. Besides, thanks to their acidic characteristics, the hydroxyl groups detected on the biochar surface by spectroscopic analysis may boost the occurrence of char-forming phenomena along the decomposition of the polymer matrix. Finally, as also reported

in the literature, Fe, P, Si, and Ca species can catalyze the production of char in synergy with the other acidic moieties, accelerating dehydration reactions [52].

The design of materials containing HTL biochar derived from municipal sludge should take into account that the composition of the feedstock is subject to variations depending on the location and time of collection [38]. While the HTL operating conditions are expected to play a major role in determining the composition and surface features of the solid product, the possibility of some differences linked to the feedstock cannot be excluded.

3.2. Screening of epoxy composites

To examine the effect of the addition of biochar on the main characteristics of the epoxy resin, four composites were prepared by adding 10 wt.% of each biochar sample to the matrix. The FTIR spectra of these composites (named EC 300-10, EC 300-30, EC 350-10, and EC 350-30) are shown in Figure S3, along with that of the cured epoxy matrix (E), as a reference. The successful curing process of all materials is attested by the disappearance of the characteristic signals of the epoxy ring (at 970, 912 and 870 cm^{-1}), which are visible in the spectrum of DGEBA (uncured resin, Figure S4), and by the intense O–H stretching band around 3400 cm^{-1}, showing up as a result of the ring opening during the curing reaction. The IR spectra of the biochar-containing composites appear identical to that of E, indicating that the fillers do not cause any chemical modification of the polymer matrix. As the main vibrational bands of the biochar overlap with intense signals of the polymer chains, the only evidence of the presence of filler particles is the band at 466 cm^{-1}, due to bending of Si–O–Si units.

The results of TGA carried out in nitrogen and air on bare epoxy resin and the four biochar-filled samples are shown in Figure S5a-d and summarized in Table S5. Comparing the $T_{5\%}$ values, it can be seen that the decomposition in nitrogen tends to start at a lower temperature in the presence of biochar, possibly because the weak acidic character of the biochar favors the dehydration and charring of the matrix. On the other hand, in air, the resin containing Ch_300-30 gives the highest $T_{5\%}$ value, indicating a good thermo-oxidative stability in the initial decomposition stage. All profiles are characterized by a main decomposition step around 350 °C, which agrees well with the behavior of similar aliphatic epoxy systems described in the literature [53]. The composites show larger residual mass at 800 °C than the bare resin in both atmospheres, which is ascribed to the formation of a thermally resistant char that lowers the heat transfer coefficients, besides the contribution of the ceramic component of biochar. In pyrolytic conditions, the final residue of the composite embedding Ch_300-30 is the highest (Table S5), indicating a considerably improved thermal stability, while in air, Ch_350-10 provides the highest residual mass. The effectiveness of these two samples in enhancing the thermal behavior of the epoxy resin could be related to the balance between an

abundance of surface functional groups, which positively affect the interactions with the polymer matrix and may foster the charring, and a substantial inorganic fraction, which can provide both thermal shielding and char-promoting effects.

DSC analysis was performed on the epoxy-biochar composites and pristine resin to verify the curing and measure the glass transition temperature (T_g). The absence of exothermic peaks associated with crosslinking reactions in the first heating ramp (see Figure S6a) indicates that the polymer network is completely cured, in agreement with the results from FTIR spectra. Figure S6b reports the DSC curves of the second heating ramp and the respective T_g values. The composites show T_g values close to that of the pristine resin (97 °C), suggesting that the addition of the biochar does not significantly alter the mobility of the polymer chains.

Based on the information gathered from the thermal analyses, Ch_300-30 was selected among the biochar samples for further experimental study, as it appears to be the best candidate for improving the thermal and thermo-oxidative stability of the epoxy resin. In the following, the EC 300-30 composite will be named "EC" for brevity, with "C" standing for the Ch_300-30 biochar. A preliminary flammability test (UL-94 vertical burning test) was performed on EC, which, like the unfilled resin, resulted as non-classifiable. Therefore, the introduction of other additives into the matrix was investigated to suppress the flammability of the system.

3.3. Functionalization and characterization of PVP-silica filler

Nonwoven mats of PVP-based electrospun fibers with a backbone of silica nanoparticles were previously shown to have multiple properties, namely low flammability, good sound absorption [18], and adsorption capacity toward organic dyes in water [54]. The excellent behavior of this material in vertical burning and smoke density tests was attributed to the high content of nanosized silica in the fibers. These results suggested the potential use of the hybrid fibers to prepare a filler that may reduce the flammability of epoxy resin in combination with HTL biochar.

To improve their dispersion and chemical affinity for the epoxy matrix, the PVP-Si fibers were functionalized first with GPTMS (G-PVP-Si) and then with the curing agent used for the resin, IPDA (GI-PVP-Si). The FTIR spectra of the samples before and after functionalization (Figure 4a) prove the successful linking of both molecules to the fibers. The spectrum of the PVP-Si fibers is characterized by a broad O–H stretching band (around 3446 cm^{-1}), due to the highly hydroxylated sol-gel-derived silica particles that fill the polymeric fibers, the stretching of the carbonyl group of PVP, at 1700 cm^{-1}, and the asymmetric band related to Si–O–Si stretching, around 1100 cm^{-1} [18]. The condensation of GPTMS with the silanol groups of PVP-Si leads to an increase in intensity of the Si–O–Si stretching band, with respect to the C=O band, and to the appearance of the bands at 761

and 912 cm^{-1} in G-PVP-Si, both related to the free epoxy rings of the silane. These latter decrease after contact with IPDA, pointing to a ring-opening reaction by the amino groups. A contribution of N–H stretching can also be seen in the GI-PVP-Si spectrum at about 3300 cm^{-1}.

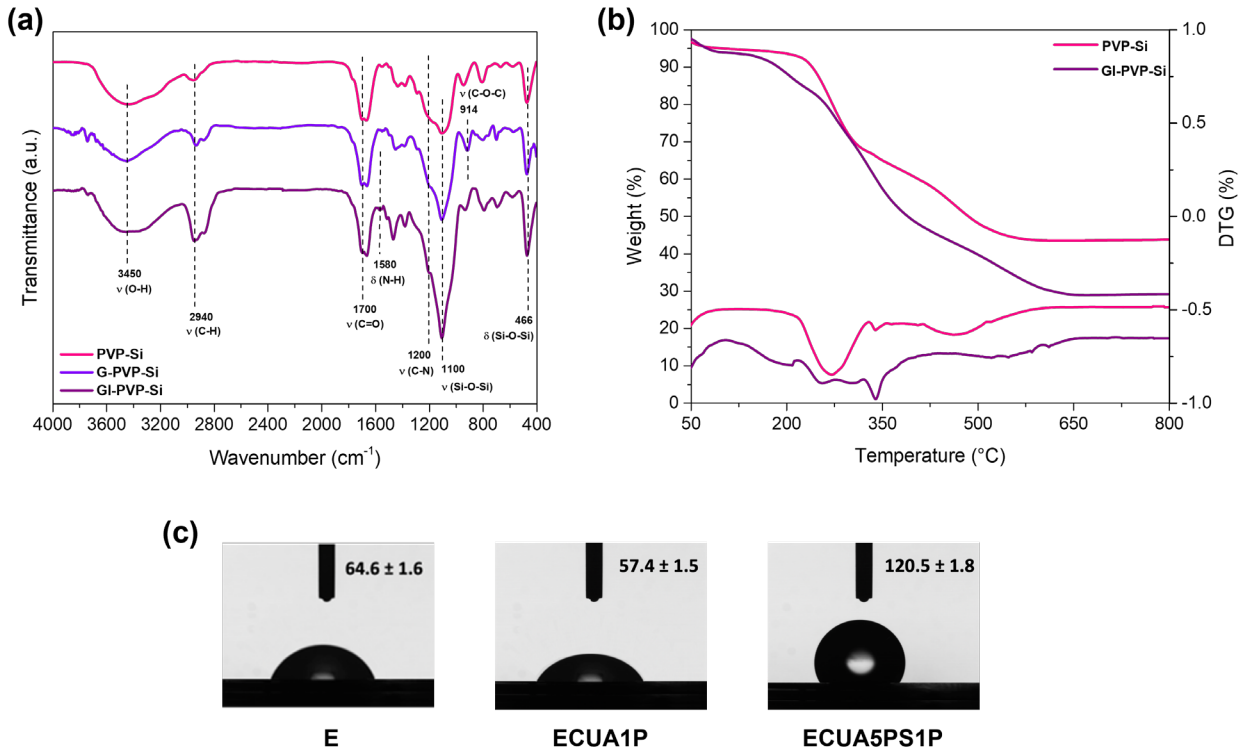

Figure 4. Characterization of PVP-Si filler: FTIR spectra of PVP-Si, G-PVP-Si, and GI-PVP-Si (a) and TGA curves of PVP-Si and GI-PVP-Si recorded in air with the corresponding derivative TG curves (b). Water contact angles (θ) of epoxy resin (E) and composite samples ECUA1P and ECUA5PS1P (c).

The effective functionalization is confirmed by comparing the TGA profiles of PVP-Si and GI-PVP-Si (Figure 4b). The samples show a limited mass loss (5 wt.%) below 100 °C, due to the removal of adsorbed water. The two mass loss steps of PVP-Si between 200 and 500 °C are associated with the thermo-oxidative decomposition of PVP, along with the condensation and sintering of the silica particles within the fibers [18]. The final residue of approximately 45 wt.% corresponds to the silica content in the pristine material. The decomposition of GI-PVP-Si starts at a lower temperature (the $T_{10\%}$ is 180 °C vs. 240 °C for PVP-Si), which can be attributed to the limited thermal stability of the introduced organosilane chains, bonded with IPDA, and of residual methoxy groups of GPTMS [55]; it also stretches over a wider range, up to 600 °C. The difference in the thermal profile (also highlighted by the derivative TG curves in Figure 4b) and overall mass loss (15 wt.% higher than that of PVP-Si), related to the organic component of the sample, gives further evidence of the successful linkage of GPTMS and IPDA on the surface of the electrospun fibers. The final SiO_2 content in GI-PVP-Si can be estimated as 30 wt.%.

The SEM images (Figure 1) of the original PVP-Si fibers and GI-PVP-Si powders obtained by milling after the functionalization show a clear change in morphology. The electrospun material is a network of long randomly oriented fibers, while the latter sample mainly consists of particles with a morphology that can be described as rods (some of them slightly bent) or whiskers. Their mean diameter is (1.8 ± 0.6) μm, while their length varies in a relatively large range, with a mean of (7 ± 3) μm. Some heterogeneous particle aggregates can also be seen. The functionalization induced some segments of the fibers to crosslink, as sketched in Figure 1, and increased their rigidity, facilitating their reduction into small particles. Indeed, the PVP-Si mats are soft and porous and tend to be compressed rather than fragmented under ball milling, while dried GI-PVP-Si samples were easily turned into a powder. GI-PVP-Si samples have a better affinity to the cured epoxy resin, resulting from the bonding of IPDA, compared to the hydrophilic untreated fibers. Owing to the size reduction (high interfacial surface area) and chemical compatibilization, the dispersion of the silica-based filler in the epoxy matrix was significantly improved, as can be seen from pictures of composites obtained by adding either PVP-Si fibers or GI-PVP-Si powders (Figure S7).

The whisker-like particles maintain a partially acidic character due to the hydroxyl-rich silica structure, which can promote the dehydration and carbonization of the polymer matrix and the formation of a stable ceramic char residue during combustion [56]. It is worth noting that the proposed treatment could be applied either to PVP-Si composite blankets recovered after their use or to small scraps derived from the electrospinning process for the manufacturing of the fibrous material.

3.4. Surface wettability of epoxy composites

To evaluate the wettability of the epoxy formulations and the influence of additives on their surface characteristics, the static water contact angle (θ) was measured on representative samples. A surface can be categorized as hydrophilic ($\theta < 90°$) or hydrophobic ($\theta > 90°$), while extremely hydrophobic surfaces provide a water contact angle ≥ 150° [57]. As it is possible to observe in Figure 4c, the epoxy resin and ECUA1P composite (containing biochar, urea, and APP) have a hydrophilic surface. The incorporation of PVP-Si whiskers into ECUA5PS1P causes a large increase in the water contact angle, meaning a lower wettability for the composite surface. While APP, urea, and biochar have a hydrophilic chemical nature, PVP-Si whiskers show a more hydrophobic character, due to the functionalization with IPDA (Figure 1). However, the surface of these whiskers is not fully coated by IPDA (see section 3.3); therefore, they are still characterized by residual polar moieties (i.e., hydroxyl groups), possibly driving the migration of some silica-based microparticles at the interface with air [46]. The functionalization with IPDA provides the PVP-Si whiskers with hydrophobic features, while their inherent fibrous morphology is responsible for the formation of a slightly rougher surface

for ECUA5PS1P compared to that of E. Finally, the wettability of the composite surface seems to be affected by the exposure of the well-tailored whiskers, conferring both chemical and morphological contributions to the higher hydrophobicity of ECUA5PS1P, with respect to pristine resin and ECUA1P (Figure 4c) [58]. These hydrophobic features of ECUA5PS1P enable its potential application as waterproof membranes or protective coatings for building materials.

3.5. Flammability, thermal and fire behavior of epoxy composites

Epoxy composites were prepared using the selected biochar (Ch_300-30, 10 wt.%) and the GI-PVP-Si whisker particles. UL-94 vertical burning tests were performed on pristine resin and the epoxy composites listed in Table S6 to investigate their flammability behavior. The unfilled epoxy system could not be classified because the specimen captured the flame after the first application of the Bunsen burner and burned completely, dripping as it burned. Similarly to E, it was not possible to classify the formulations containing only HTL-derived biochar or PVP-Si particles, though these latter did not drip during combustion. However, EC5PS shows lower flammability compared to E, EC, and E5PS, probably ascribed to the combined char-forming character of additives causing the formation of a carbonaceous material able to act as an effective barrier toward the release of flammable gases [33,49,59]. Then, small amounts of urea (2 wt.%) and APP (3 wt.%) were also added to the epoxy systems. Looking at EUA5PS1P, urea and APP promote a decrease in the t_1 after-flame times (Table S6), due to the flame retardant action of these compounds during the early combustion stages and along the burning process. Particularly, the decomposition of APP generates acid phosphorus compounds promoting the dehydration of the polymer matrix and the consequent char formation, while the degradation of urea mainly produces nitrogen, exerting a dilution effect in the gas phase [60].

The addition of the biochar into EUA5PS1P sample allows for obtaining a formulation that exhibits no dripping V0 rating (Table S6 and Table 2), even at a very low P loading (i.e., 1 wt.%), due to a synergistic condensed phase action of the waste-derived material with the other additives during the combustion [61]. Concerning ECUA5PS1P, the use of biochar and a specific amount (i.e., 5 wt.%) of PVP-Si particles, together with urea and APP, is fundamental to significantly reduce the after-flame times along the whole test and give rise to a residual char with a coherent and continuous structure (Table S6). The flame retardant effectiveness of urea arises from its multifunctional role as a heat sink, gas-phase diluent, and char-forming synergist, particularly when used in combination with APP and carbonaceous fillers. It is reported that this synergistic behavior enhances flame retardancy without significantly compromising the processing or mechanical performance of the polymer composite [42,62].

Since the whiskers mainly consist of silica nanoparticles, their decomposition generates refractory material at the surface (see section 3.3), while their slightly acidic nature boosts the dehydration of the epoxy matrix to produce a large amount of ceramic char. Unlike the biochar obtained at higher temperature (350 °C), the one used for the preparation of ECUA5PS1P exhibits more hydroxylated surface and thus can promote the occurrence of charring processes. These flame retardant mechanisms, taking place during the combustion of the self-extinguishing sample (ECUA5PS1P), cause an increase in the melt viscosity of the burning system and the generation of a stable char, rich of silicon-based species (see section 3.5), acting as an oxygen barrier and thermal shield for the underlying polymer [63].

In view of the outcomes related to the flammability tests, only the thermal properties, mechanical response, and fire behavior of the self-extinguishing system and some other counterparts (E, EC, E5PS, and EC5PS) will be discussed to show the influence of each component on the performance of the final product. LOI measurements were carried out on the above-selected samples (E, EC, E5PS, EC5PS, and ECUA5PS1P) and ECUA3PS1P to evaluate the minimum percentage of oxygen needed to sustain the candle-like combustion after ignition in an O_2/N_2 mixture. Table S7 shows that the right amount and concurrent presence of PVP-Si whiskers, biochar, urea, and APP effectively slow down the candle-like combustion. The highest value of LOI is observed for ECUA5PS1P, surpassing ECUA3PS1P, which could only achieve V1 rating in UL-94 vertical burning tests, thus confirming that a certain content of GI-PVP-Si is important for enhancing the flame retardant behavior. These results well agree with the outcomes of the UL-94 vertical flame spread tests.

The thermal decomposition profiles of pristine epoxy and epoxy composites are reported in Figures 5a-d. All the samples exhibit the main decomposition step at ~350 °C. The presence of hydroxyls and other oxygen-containing functional groups on the surface of PVP-Si whiskers and HTL-derived biochar particles confers acidic characteristics. These chemical features favor the carbonization process through the dehydration of epoxy resin [64–66], resulting in an anticipated mass loss (see $T_{5\%}$ in Table S8) for EC and E5PS compared to E. This effect is particularly evident in the case of EC, as the use of biochar particles also leads to an increase (10 wt.%) in the residual mass at 800 °C, compared to the counterpart resulting from the pyrolytic decomposition of the pristine system (Table S8). On the other hand, PVP-Si whiskers have a slightly weaker effect on the carbonization process because the PVP film covers the silica nanoparticles and their surface hydroxyl groups. [54]. However, the pyrolysis of PVP-Si whiskers contributes forming an abundant ceramic char when the microstructures are employed in combination with biochar particles. Indeed, EC5PS shows very good thermal stability, as both its $T_{5\%}$ and residual mass at 800 °C are higher than those of E (Table S8). The addition of APP and urea into EC5PS does not affect the residue but causes an anticipation of

$T_{5\%}$, probably ascribed to their decomposition that releases acidic phosphorus compounds and non-flammable volatiles (i.e., N_2 and phosphorus species) [33,62].

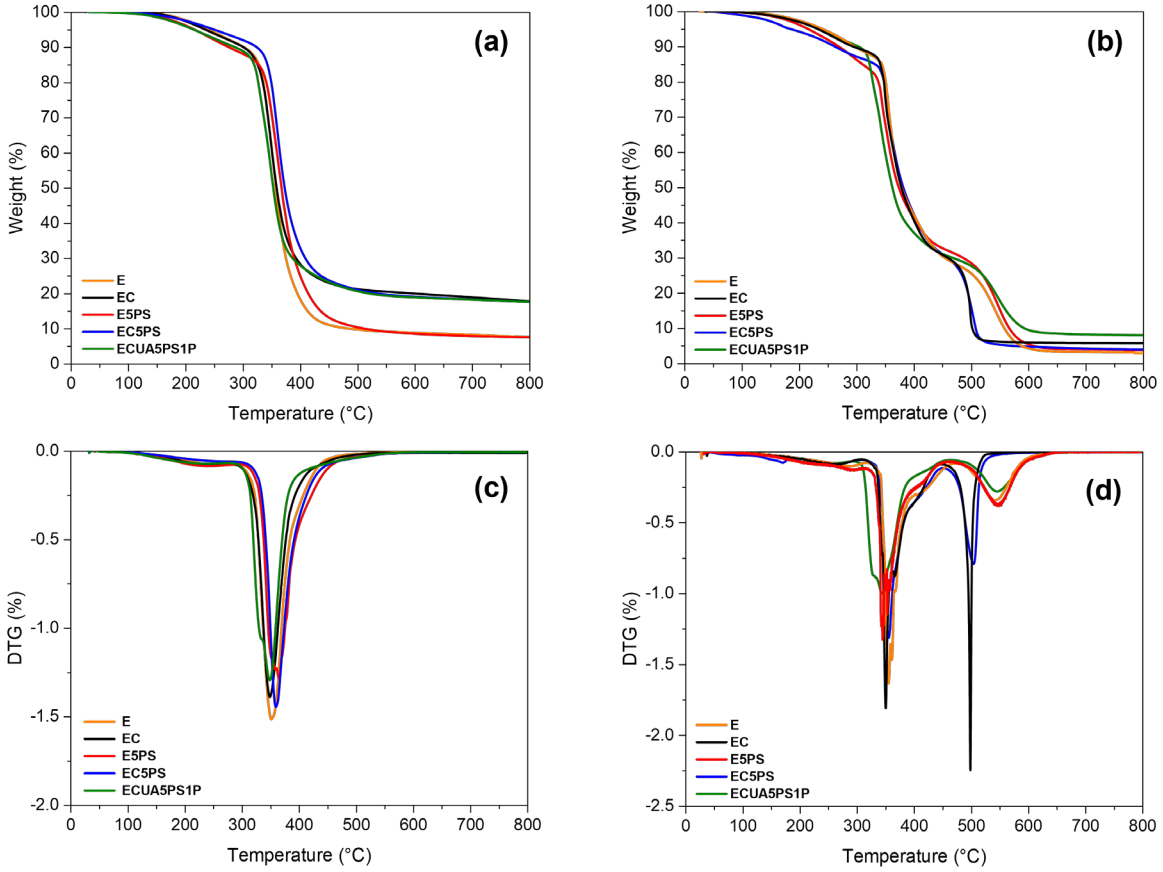

Figure 5. TGA curves (a, b) and DTG curves (c, d) of pristine resin and epoxy composites recorded under N_2 (a, c) and air (b, d).

Figures 5b,d show the thermogravimetric data collected in air. Looking at EC, the results confirm the char-forming behavior of the biochar particles, which allows for a higher (6 wt.%) residual mass compared to the one (3 wt.%) of E (Table S8). The presence of metal species in the waste-derived biochar additionally boosts the charring phenomena taking place during the combustion of composites containing such an additive [52]. The good thermo-oxidative stability of ECUA5PS1P rises from the combined use of APP, urea, PVP-Si whiskers, and biochar particles. The additives enable a significant increase in T_{max2}, which means that the heat exchange at the boundary phase between the gas phase and the polymer bulk is limited, and the highest residual mass is produced at 800 °C (Table S8). This effect on the thermo-oxidative stability of ECUA5PS1P may be due not only to the char-forming character of the biochar particles and acidic phosphorus compounds, but also to other mechanisms taking place during the combustion, namely: (i) the decomposition of APP and urea in air forms nitrogen able to disrupt the diffusion of oxygen; (ii) the degradation of PVP-Si

whiskers produces a huge amount of refractory silica nanoparticles, which promote the generation of a stable aromatic char able to prevent the diffusion of flammable gases and oxygen from the surroundings into the material, and act as effective thermal shield and barrier [67,68].

Figures S8a,b displays the DSC curves of the unfilled resin and epoxy composites. It is possible to observe that the first heating ramp does not show any presence of residual exothermic peak, confirming the completeness of the curing process for all the investigated samples in the adopted experimental conditions. These results agree with the outcomes of FTIR analyses. Overall, Figure S8b reveals that the glass transition temperatures of all systems are not significantly changed compared to that of the pure epoxy resin.

PCFC measurements prove that the inclusion of the HTL-derived biochar into the epoxy resin causes the most significant increase in the residual char (Table S9, Figure 6a). The biochar has a crucial role in the condensed phase; indeed, as mentioned above, it acts as a char-former, thanks to the hydroxyl groups present on its surface, and slows down the oxidative degradation of the polymer matrix [33]. As attested by the significant decrease in pHRR (13%), HRC (13%), and THR values (19%) compared to the pristine resin (Table S9), PCFC tests performed on ECUA5PS1P highlight that the biochar, in synergy with GI-PVP-Si whisker particles, APP, and urea, limits the oxygen diffusion and thus affects the heat release parameters [69,70]. Finally, the highest residue recorded for ECUA5PS1P, together with the anticipation of the initial decomposition stage at a very low temperature, with respect to the unfilled systems as benchmark (Table S9, Figure 6a), clearly suggest a strong condensed phase action of all the additives.

Figure 6b and Table 2 show the results from the cone calorimetry tests. The data confirm the char-forming character and dehydrating effect exerted by the GI-PVP-Si whisker particles and biochar during the burning, as all the epoxy formulations containing both fillers, even alone, give lower TTI and higher residues with respect to the pristine resin. While the weak acidic nature of these fillers is mainly responsible for an anticipated ignition, the ceramic component of whisker particles and the high thermal stability of the biochar favour the formation of higher amounts of residual char, due to the thermal barrier action slowing down the heat exchange and the oxygen diffusion at the boundary phase (Table 2) [71,72].

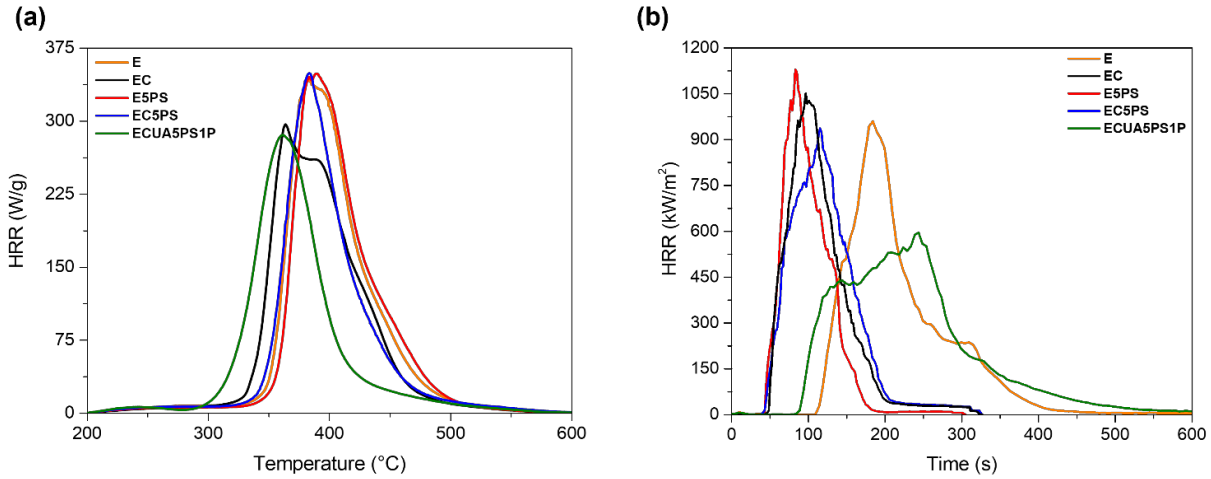

Figure 6. HRR vs. time of pristine resin and epoxy composites measured by PCFC (a) and cone calorimetry tests (b).

Table 2. Results obtained from cone calorimetry and UL-94 vertical burning tests for the investigated epoxy systems.

Sample	TTI (s)	THR (MJ/m²)	ΔTHR (%)	pHRR (kW/m²)	ΔpHRR (%)	Residue (wt.%)	TSR (m²/m²)	ΔTSR (%)	UL-94/dripping
E	109 ± 2	106 ± 9	-	961 ± 101	-	3 ± 0.1	3432 ± 33	-	NC/yes
EC	45 ± 1	82 ±1	–23	1051 ± 95	+9	8 ± 0.1	3789 ± 17	+10	NC/no
E5PS	42 ± 15	71 ± 13	–33	1131 ± 97	+17	6 ± 0.2	3043 ± 96	–11	NC/no
EC5PS	42 ± 8	85 ± 1	–19	937 ± 141	–2	10 ± 1	3595 ± 27	+5	NC/no
ECUA5PS1P	80 ± 11	109 ± 7	+2	619 ± 61	–36	11 ± 1	3083 ± 56	–10	V0/no

TTI = Time To Ignition, **TTFO** = Time To Flame Out**, THR** = Total Heat Release, **HRR** = Heat Release Rate, **pHRR** = peak Heat Release Rate, **TSR** = Total Smoke Release

Looking at Figure 6b, E5PS shows the sharpest curve with the highest pHRR, which is probably ascribed to the non-charring and highly flammable PVP. The addition of the biochar into E5PS mitigates such an effect on the heat release rate, limiting the heating diffusion along the epoxy matrix. The incorporation of APP and urea into EC5PS results in a broadening of the heat release rate curve, revealing a slower heat release over a longer timespan for ECUA5PS1P compared to the blank epoxy (Figure 6b). The endothermic decomposition of APP and urea causes the release of phosphorus radicals and nitrogen, resulting in higher TTI value for ECUA5PS1P than EC, E5PS, and EC5PS. The phosphorus radicals poison the oxygen radicals in the flame (i.e., acting as radical scavengers), while nitrogen dilutes the flammable volatiles in the gas phase [73]. Urea decomposes under heat releasing nitrogen, which reduces the oxygen concentration in the atmosphere surrounding the polymer bulk, thus decreasing the amount of species sustaining the flame. Moreover, nitrogen can absorb part of the heat radiation, lowering the temperature of the gas phase and thus inhibiting the production of flammable species by thermal feedback. The combination of nitrogen dilution and

reduced oxygen availability in the gas phase contributes to the self-extinguishing behavior of ECUA5PS1P and the lowest value of pHRR, which is 36% lower than that of E (Table 2).

The decomposition of APP generates acidic phosphorus compounds, which enhance the charring of the polymer matrix during combustion. This contributes to the condensed phase action of the GI-PVP-Si whisker particles and the biochar, giving rise to the formation of a stable char able to adsorb gases (e.g., phenol, cresol, carbon dioxide, naphthalene, anthracene, among others) and limit the emission of volatile acid compounds. This may explain the lowest values of TSR and SEA collected for ECUA5PS1P, which are up to 18% lower than those of E (Table 2 and Table S10). Finally, it is worth mentioning that the presence of metallic species in the HTL-derived biochar (Table S2) may catalyze the charring of the organic polymer matrix, well supporting the higher amounts of residual char formed after the burning of EC, EC5PS, and ECUA5PS1P, with respect to the other formulations (Table 2). In many applications of HTL-derived biochar (e.g., wastewater treatment), metallic impurities can have a negative impact on the process and raise pollution concerns. In this case, however, these impurities are a functional component. [74]. In view of the above results, a simplified flame retardant mechanism is proposed (Figure 7), which illustrates the phenomena occurring along the combustion of all the prepared formulations.

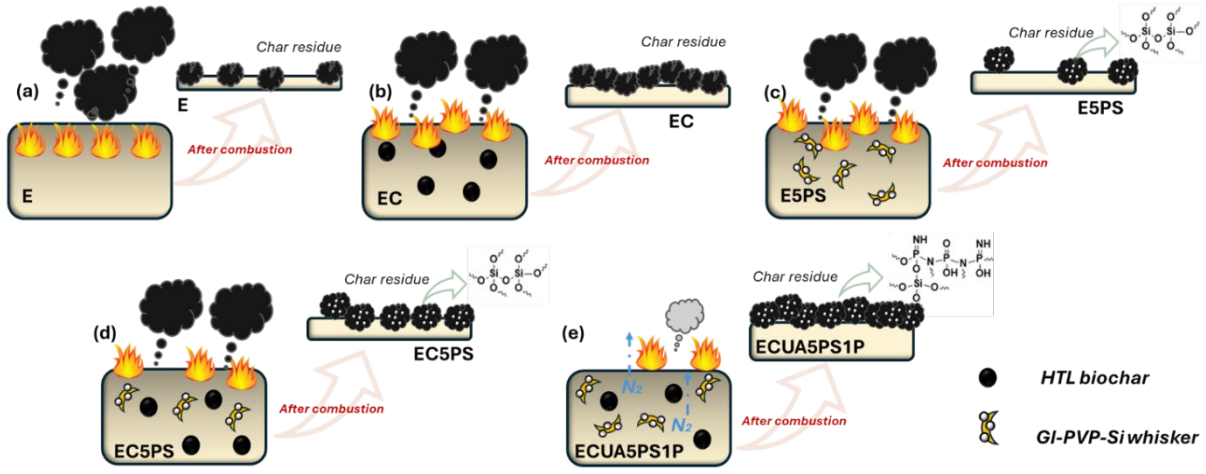

Figure 7. Proposed condensed phase mechanism of epoxy composites in oxygen atmosphere. (a) E, (b) EC, (c) E5PS, (d) EC5PS, (e) ECUA5PS1P. The advanced stage of the decomposition of the polymer matrix is illustrated in the dark yellow region. The chemical structures describe the polymeric substructures formed in the respective carbonaceous residue surface.

To explore more deeply in the condensed phase, SEM-EDX measurements (Figure S9 and Table S11) were performed on residual chars to highlight the differences in terms of chemical composition and morphologies among the burned materials derived from the pristine system and its composites after UL-94 vertical flame spread tests. Figure S9 shows that the residual char of E is characterized by some small holes and thin cracks that facilitate the release of flammable volatiles to the gas phase

during the combustion (Figure 7a). The addition of biochar into the epoxy matrix (EC) causes the formation of a jagged continuous char (Figure S9), limiting heat and mass transfer thanks to its tortuous morphology (Figure 7b). Compared to the one generated from E, the residual char obtained from the combustion of E5PS appears more compact and coherent, although several holes are present. The compactness may be ascribed to the whisker particles giving rise to a ceramic char with silica substructures (Si–O–Si, Figure 7c, Table S11). On the other side, the presence of PVP in the matrix causes the generation of bubbles, made of flammable gases, which hinder the formation of a continuous char, well supporting the poor fire behavior of E5PS [17]. The incorporation of GI-PVP-Si whisker particles into EC (EC5PS) provides compactness to the char of EC, and thus the carbonaceous residue appears free of cracks and holes, confirming the crucial role of the HTL-derived biochar in the condensed phase, especially in synergy with the inorganic filler (Figures S9 and 7d). The combined use of whisker particles, biochar, APP, and urea accounts for the formation of a slightly intumescent and swollen multicellular char characterized by the presence of P–N–O–Si–O–P polymeric substructures (Figures S9 and 7e) on the surface, as confirmed by the high retentions of P and N (Table S11). The decomposition of urea releases NH_3 that reacts with polyphosphoric acids to give P–N–O substructures (e.g., phosphorus oxynitride) [75], which can consequently condense with the silanol groups of Si–O–Si and P–O–Si polymeric species to generate a thermally stable residue [76]. This char works as an effective thermal shield and oxygen barrier at the boundary layer and is responsible for a delayed ignition (Table 2), compared to the other epoxy systems, and the excellent performances in the UL-94 (V0 class flammability without any dripping) and cone calorimetry tests. This strong condensed phase mechanism, in which the biochar plays a key role, may be enhanced by a slight gas phase action through active radical scavenging and dilution. Overall, each component exerts its crucial function into a clear synergistic chain enabling the construction of a dense, stable, intumescent ceramic-like char layer rich in P–N–O–Si hybrid structures, protecting the underlying polymer, and a side slight gas phase activity. PVP-Si whisker particles act as a silicon source and initial charring catalysts, while the biochar contributes giving carbon skeleton to the final thermally stable char and metal catalytic sites, promoting char-forming reactions. Simultaneously, the decomposition of APP generates: (i) polyphosphoric acids able to dehydrate the polymer matrix, (ii) ammonia as source of nitrogen (diluting the combustible volatiles in the gas phase) and former component for phosphorus oxynitrides, (ii) phosphorus radicals ($PO^{\bullet}$ or $HPO^{\bullet}$) working as inhibitors for oxygen radicals in the gas phase, as observed in previous research studies by gas evolved analysis [42,77]. Finally, as already stated above, urea synergizes the release of nitrogen and promotes physical crosslinking by forming, together with APP, a strong intersegmental hydrogen-bonded network with the epoxy resin.

Despite the use of an aliphatic amine as hardener (i.e., IPDA), the application of a well-designed strategy exploiting phosphorus flame retardants, nitrogen additives, and a waste-derived biochar can be a promising methodology to obtain sustainable self-extinguishing epoxy composites, even with only 1 wt.% of P in the polymer matrix. Considering the outcomes related to flammability and fire behavior, it appears clear that whisker-like particles based on tailored electrospun PVP-coated silica fibers represent the tip of the balance in the proposed flame retardant strategy. This innovative synergist, which can be easily obtained by electrospinning, without any issue linked to optimization of yield, and by using inexpensive PVP, is able to exert a strong charring effect, while providing a ceramic barrier during the burning.

3.6. Dynamic-mechanical behavior and mechanical properties of epoxy composites

DMA was performed to evaluate the viscoelastic response as a function of temperature of E and epoxy composites. The glass transition temperatures of the samples were taken from the maximum values of tan δ curves (Figure 8a). The blank epoxy shows a symmetric and narrow tan δ curve with the highest tan δ peak (at 99 °C), revealing that E can easily dissipate the application of a load by energy dissipation mechanisms (e.g., segmental motions) [78]. The incorporation of the HTL-derived biochar into the epoxy matrix (EC) leads to a material exhibiting an asymmetric and wider tan δ curve, due to a broad distribution of relaxation phenomena (Figure 8a) [33,64]. Biochar particles insert between polymer chains, shield intermolecular interactions, increase free volume, and unequivocally lower the T_g. The presence of such particles causes a plasticizing effect in the epoxy network, giving rise to a slight decrease (~4%) in the T_g and a material less able to dissipate energy. This effect on the viscoelastic behavior is also evident in E5PS, probably ascribed to the increase of filler-matrix interface defects [54]. Despite the hydroxyl groups on the surface of whiskers (see section 3.3 and Figure 4a), the compatibilization of these microstructures by IPDA makes it possible for their good dispersion throughout the polymer matrix, which explains the T_g of E5PS that is almost the same as E. The combined use of GI-PVP-Si and biochar (EC5PS) allows for the synthesis of a material giving a symmetric and narrow tan δ curve, with a T_g (96 °C) that is practically unvaried compared to E (Figure 8a). On the other side, the addition of urea and APP into EC5PS triggers again relaxation phenomena and the generation of two co-continuous phases with different chain mobilities in the polymer matrix. As reported in the literature, urea and APP can form a strong intersegmental hydrogen-bonded network with epoxy resin systems [42,79]. These intersegmental interactions, together with the establishment of hydrogen bonds between the oxygen-containing functional groups on the surface of both the biochar particles and the PVP-Si filler (see section 3.3) with the hydroxyls originated by the crosslinking process appear to lead to a second T_g (Figure 8a) [54], which is higher than that of E; thus, ECUA5PS1P displays a tan δ curve with a maximum located at 94 °C (T_{g1}) and

a shoulder at 112 °C (T_{g2}), as confirmed by the good curve fitting obtained with two overlapped peaks (Figure S10). Hydrogen bonding, as a strong secondary interaction, typically acts as a physical crosslink, restricting polymer chain segment mobility and thus tending to increase the T_g [80]. The coexistence of these hydrogen-bond-rich, interfacial domains with the bulk matrix introduces dynamic and structural heterogeneity within the composite, reflecting the presence of polymer segments experiencing different degrees of mobility and constraint, which lead to the formation of phases characterized by distinct relaxation dynamics compared to the bulk epoxy network [42,81]. Despite hydrogen bonding, the interface between the rigid biochar particles and the epoxy matrix may be imperfect (e.g., interfacial voids, stress concentration). These defects can act as initiation sites for early relaxation during thermomechanical scanning, manifesting as T_g peak broadening and a slight peak temperature decrease. The introduction of free volume by the filler is another possibility; irregularly shaped filler particles may disrupt the close packing of polymer chains, introducing extra free volume at the interface, thereby facilitating chain segment relaxation.

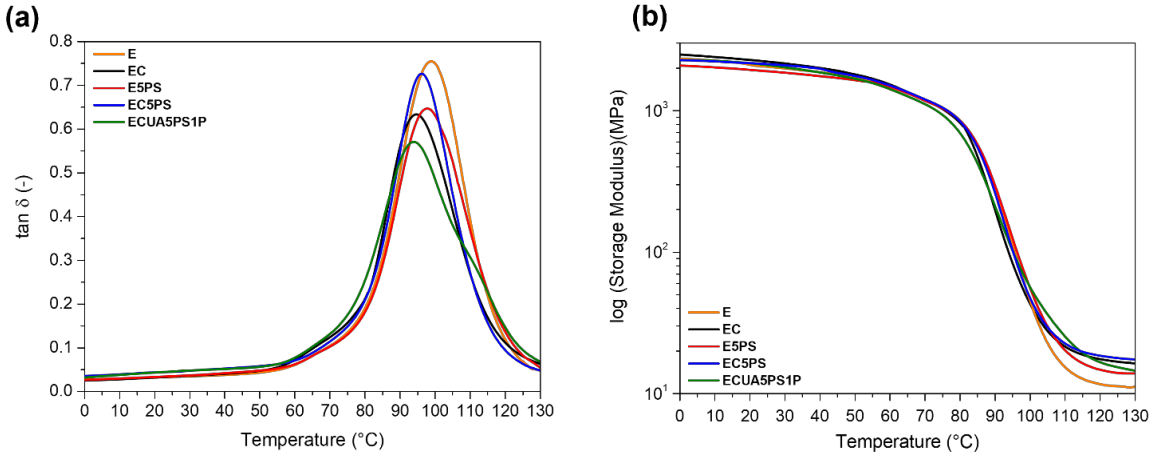

Figure 8. Mechanical damping factor (tan δ) (a) and storage moduli (E′) (b) of pristine resin and epoxy composites, collected as a function of temperature.

The hydrophilic character of PVP-Si particles (see section 3.3), composed of porous fibers embedded with sol-gel silica nanoparticles full of hydroxyl groups in their backbone, disturbs the dipole-dipole intra- and inter-macromolecular interactions between the epoxy chains: for this reason, E5PS shows the lowest value of storage modulus (E') in the glassy state region (Figure 8b), compared to the pristine system and the other composites [82,83]. Considering the other samples, the less hydrophilic nature of biochar and the hindering action of additives cause a stiffening effect on the polymer network, resulting in E' values that approach those of E. To conclude, the simultaneous use of PVP-Si and biochar is crucial to obtain final composites with very low flammability as well as good dynamic-mechanical behavior.

To shed light on the effect of the selected fillers on the mechanical properties of epoxy resin, the flexural behavior of E, EC, E5PS, EC5PS, and ECUA5PS1P was evaluated (Table 3). The presence of oxygen-containing functional groups on the surface of char particles negatively affects the flexural response of EC, as it exhibits lower modulus (E_B), fracture strength ($\sigma_{u,B}$), and elongation at break ($\varepsilon_{f,B}$) compared to the pristine resin. While the use of char particles alone is detrimental because of their polar character, the incorporation of compatibilized PVP-Si whiskers alone (E5PS) in the epoxy system leads to an improvement of the flexural modulus, with respect to EC and E (Table 3) [33,84]. This result may be ascribed to the good distribution of the microstructures in the epoxy matrix and their interaction with the crosslinked polymer chains. However, the introduction of the other additives into the resin (ECUA5PS1P) causes a decrease in the motion of the chain segments and consequently the formation of topological constraints, which result in a stiffer network (Table 3), well supporting the hinderance phenomena observed from DMA measurements [85,86]. In view of that, despite the beneficial effect of the functionalized PVP-Si whiskers on the flexural modulus of epoxy resin, ECUA5PS1P is characterized by lower E_B, $\sigma_{u,B}$, and $\varepsilon_{f,B}$ values than E5PS. Thus, the self-extinguishing material appears less ductile and more brittle.

Table 3. Flexural test results of pristine resin and epoxy composites for comparison.

Sample	Flexural Modulus (MPa)	Fracture strength (MPa)	Strain at break (%)
E	4345 ± 65	144 ± 8	3.9 ± 0.1
EC	4148 ± 26	33 ± 3	0.8 ± 0.3
E5PS	5251 ± 41	40 ± 5	0.7 ± 0.2
EC5PS	4550 ± 53	51 ± 3	1.1 ± 0.1
ECUA5PS1P	4540 ± 76	30 ± 4	0.7 ± 0.2

The decrease in toughness can be attributed to the combined effects of stiffening of the polymer matrix, a restricted plastic deformation, and a stress concentration induced by the additives. The incorporation of rigid fillers and flame retardant components (such as APP, biochar, and PVP-Si whiskers) increases the elastic modulus of the epoxy matrix, which limits energy dissipation through plastic deformation under applied stress. Indeed, ECUA5PS1P shows higher E_B compared to blank epoxy, but lower $\sigma_{u,B}$ and $\varepsilon_{f,B}$ values than pristine system (see Table 3). Also, imperfect filler-matrix interfacial adhesion and particle agglomeration can introduce stress concentration sites, facilitating crack initiation and accelerating crack propagation [87,88]. Moreover, the formation of hydrogen-bonded or highly crosslinked interfacial regions reduces chain mobility, further suppressing toughening mechanisms such as shear yielding. Collectively, these factors reduce the capability of

ECUA5PS1P in absorbing and dissipating mechanical energy, resulting in a significant decrease in toughness.

Overall, the above outcomes highlight the strong potential of the developed epoxy composites for multifunctional integration, as good performances of fire safety, moisture/water resistance, and mechanical behavior can be simultaneously satisfied. The achievement of V0 rating in UL-94 flame spread tests, combined with a highly hydrophobic surface (with water contact angle ~120°), and good thermomechanical properties, demonstrates that the synergistic incorporation of APP, urea, biochar, and PVP-Si whiskers enables functionalities that are often difficult to design within a single material system. Such a combination of properties makes these materials particularly attractive for applications requiring integrated fire resistance, environmental durability, and lightweight construction, including transportation interiors (e.g., rail, aerospace, and automotive components), electronic device encapsulation, housing exposed to thermal and humidity stresses, and protective or insulating components for energy storage and power management systems.

4. Conclusions

This study presents a novel waste-to-wealth approach for valorizing the solid residue produced by HTL of sewage sludge, employing it as a functional additive in epoxy-based composites. The HTL-derived biochar, characterized by high inorganic content and a hydroxyl-rich surface, can effectively interact with the epoxy matrix. Among the four different biochar samples evaluated, one was identified as particularly suitable for flame retardant applications (biochar obtained at 300 °C and 30 min), due to its ability to confer enhanced thermal stability to the resin, without adversely affecting its viscoelastic properties, even at a significant loading of 10 wt.%. However, the integration of other additives into the polymer matrix was needed to provide the composites with self-extinction. To this aim, PVP-coated silica fibers produced by electrospinning were reduced to powder and functionalized to obtain whisker-like microparticles that were uniformly dispersed in the epoxy resin. The combination of these tailored silica-based particles with biochar, along with small amounts of urea and APP, resulted in composites that attained a V0 rating in UL-94 vertical flame spread tests, even with only 1 wt.% of P loading. Compared to the pristine epoxy system, final composites showed a notable reduction in the peak of heat release rate and in the total smoke release, ~36% and ~10%, respectively.

These enhanced flame retardant properties can be attributed to the effects among the additives during combustion. Thanks to their surface acidity, both biochar and PVP-coated silica fibers synergistically promote the dehydration of the polymer matrix and the formation of a continuous and stable ceramic-like char layer, effectively hindering the diffusion of heat, oxygen, and smoke. Simultaneously, urea

and APP provide a moderate gas phase effect through the release of nitrogen and phosphorus species, quenching oxygen radicals in the flame. Importantly, the resulting composites retain mechanical and thermal integrity, with glass transition temperature and flexural modulus remaining nearly unchanged with respect to the pristine resin. However, the presence of fillers negatively affects both the flexural strength and the strain at break of final composites. In addition, the incorporation of functionalized silica whiskers imparts surface hydrophobicity (with contact angles up to ~120°) to the material, suggesting potential use in multifunctional applications requiring both fire and water resistance. The proposed composite formulation may represent a promising platform for the design of next-generation multifunctional polymer materials tailored to demanding safety-critical applications.

Overall, this work demonstrates the feasibility of a dual waste valorization pathway in which sewage sludge can be used as both a feedstock for biocrude production and a source of valuable solid co-products. The unique physicochemical properties of HTL-derived biochar offer new possibilities for the development of sustainable materials. Future research could investigate how different sewage sludge sources influence biochar functionality, as well as exploring additional applications such as environmental remediation through the removal of water contaminants. Defining utilization options for this solid product prevents its landfilling or incineration, enables medium-term carbon sequestration and improves resource cycling, with consequent environmental as well as economic benefits. It is envisaged that the integration of such model of co-product management in the HTL process would ultimately promote its implementation in biorefineries.

CRediT authorship contribution statement

Immacolata Mazzuoccolo: Investigation, Formal analysis, Visualization. **Immacolata Climaco**: Investigation, Formal analysis, Visualization. **Jessica Passaro:** Investigation, Formal analysis. **Francesca Di Lauro**: Investigation, Writing – original draft. **Daniele Battegazzorre:** Investigation. **Milijana Jovic**: Investigation. **Pietro Russo:** Validation, Supervision. **Giulio Malucelli:** Validation, Supervision, Writing – review & editing. **Sabyasachi Gaan**: Validation, Supervision, Writing – review & editing. **Antonio Aronne**: Validation, Supervision, Writing – review & editing. **Fabio Montagnaro:** Validation, Writing – review & editing. **Marco Balsamo:** Methodology, Supervision, Project administration, Funding acquisition, Writing – review & editing. **Claudio Imparato**: Formal analysis, Project administration, Conceptualization, Funding acquisition, Writing – original draft, Writing – review & editing. **Aurelio Bifulco**: Formal analysis, Methodology, Project administration, Conceptualization, Funding acquisition, Writing – original draft, Writing – review & editing.

Declaration of competing interest

The other authors declare that they have no known competing financial interests or personal relationships that could have appeared to influence the work reported in this paper.

Funding Sources

This research work was partially funded by the Project "Eco-sustainable Production of bIofuels from the Conversion of sludges through hydrothermal liquefaction" (EPIC), Programma per il Finanziamento della Ricerca di Ateneo (FRA) 2022 of the University of Naples Federico II, and by the Project funded under the National Recovery and Resilience Plan (NRRP), Mission 4 Component 2 Investment 1.3 - Call for tender No. 1561 of 11.10.2022 of Ministero dell'Università e della Ricerca (MUR); funded by the European Union – NextGenerationEU, Project code PE0000021, Project title "Network 4 Energy Sustainable Transition – NEST".

Acknowledgements

The authors thank Maria Cristina Del Barone, in charge of LaMest (SEM and TEM laboratory) at Polymers Composites and Biomaterials Institute of National Research Council (IPCB-CNR, Pozzuoli, Naples), and Francesco Saverio Esposito (University of Naples Federico II) for the experimental support.

References

[1] Y. Zhou, B. Gu, The impacts of human activities on Earth Critical Zone, Earth Crit. Zo. 1 (2024) 100004. https://doi.org/10.1016/j.ecz.2024.100004.

[2] K. Kümmerer, J.H. Clark, V.G. Zuin, Rethinking chemistry for a circular economy, Science. 367 (2020) 369–370. https://doi.org/10.1126/science.aba4979.

[3] Bańkowski, K., Ferdinandusse, M., Hauptmeier, S., Jacquinot, P., Valenta, V. The macroeconomic impact of the Next Generation EU instrument on the euro area. European Central Bank, ECB Occasional Paper No. 255, 2021.

[4] Z. Qu, K. Wu, E. Jiao, W. Chen, Z. Hu, C. Xu, J. Shi, S. Wang, Z. Tan, Surface functionalization of few-layer black phosphorene and its flame retardancy in epoxy resin, Chem. Eng. J. 382 (2020) 122991. https://doi.org/10.1016/j.cej.2019.122991.

[5] S. Wi, S. Yang, Y.U. Kim, Y. Kang, S. Kim, Toxicity characteristics and fire retardant performance of commercially manufactured organic insulation materials for building applications, Constr. Build. Mater. 341 (2022) 127898. https://doi.org/10.1016/j.conbuildmat.2022.127898.

[6] T. Thevega, J. Jayasinghe, D. Robert, C.S. Bandara, E. Kandare, S. Setunge, Fire compliance of construction materials for building claddings: A critical review, Constr. Build. Mater. 361 (2022) 129582. https://doi.org/10.1016/j.conbuildmat.2022.129582.

[7] J.C. Markwart, A. Battig, L. Zimmermann, M. Wagner, J. Fischer, B. Schartel, F.R. Wurm, Systematically Controlled Decomposition Mechanism in Phosphorus Flame Retardants by Precise Molecular Architecture: P–O vs P–N, ACS Appl. Polym. Mater. 1 (2019) 1118–1128. https://doi.org/10.1021/acsapm.9b00129.

[8] J. Zhang, Y. Guo, W. Shao, F. Xiao, Benign design of intumescent fire protection coatings for steel structures containing biomass humic acid as carbon source, Constr. Build. Mater. 409 (2023) 134001. https://doi.org/10.1016/j.conbuildmat.2023.134001.

[9] J. Su, A. Bloodworth, Simulating composite behaviour in SCL tunnels with sprayed waterproofing membrane interface: A state-of-the-art review, Eng. Struct. 191 (2019) 698–710. https://doi.org/10.1016/j.engstruct.2019.04.067.

[10] C. Baoyu, C. Jiehu, L. Chang, F. Jiamin, W. Shuxia, D. Xiuhong, L. Zhen, Synthesis of MgAl-LDH from three alkali sources for boosting flame retardancy of EP with APP, Constr. Build. Mater. 447 (2024) 137997. https://doi.org/10.1016/j.conbuildmat.2024.137997.

[11] P. Sun, H. Zhang, Y. Leng, Z. Wang, J. Zhang, M. Xu, X. Li, B. Li, Construction of flame retardant functionalized carbon dot with insulation, flame retardancy and thermal conductivity in epoxy resin, Constr. Build. Mater. 451 (2024) 138853. https://doi.org/10.1016/j.conbuildmat.2024.138853.

[12] H. Vahabi, H. Wu, M.R. Saeb, J.H. Koo, S. Ramakrishna, Electrospinning for developing flame retardant polymer materials: current status and future perspectives, Polymer (Guildf). 217 (2021) 123466. https://doi.org/10.1016/j.polymer.2021.123466.

[13] E. Gallo, Z. Fan, B. Schartel, A. Greiner, Electrospun nanofiber mats coating-new route to flame retardancy, Polym. Adv. Technol. 22 (2011) 1205–1210. https://doi.org/10.1002/pat.1994.

[14] N. Bhardwaj, S.C. Kundu, Electrospinning: A fascinating fiber fabrication technique, Biotechnol. Adv. 28 (2010) 325–347. https://doi.org/10.1016/j.biotechadv.2010.01.004.

[15] M.I. Loría-Bastarrachea, W. Herrera-Kao, J. V. Cauich-Rodríguez, J.M. Cervantes-Uc, H. Vázquez-Torres, A. Ávila-Ortega, A TG/FTIR study on the thermal degradation of poly(vinyl pyrrolidone), J. Therm. Anal. Calorim. 104 (2011) 737–742. https://doi.org/10.1007/s10973-010-1061-9.

[16] T.E. Newsome, S. V Olesik, Electrospinning silica/polyvinylpyrrolidone composite nanofibers, J. Appl. Polym. Sci. 131 (2014) 40966. https://doi.org/10.1002/app.40966.

[17] A. Bifulco, I. Climaco, A. Casciello, J. Passaro, D. Battegazzore, V. Nebbioso, P. Russo, C. Imparato, A. Aronne, G. Malucelli, Prediction and validation of fire parameters for a self-extinguishing and smoke suppressant electrospun PVP-based multilayer material through machine learning models, J. Mater. Sci. 60 (2024) 1019–1040. https://doi.org/10.1007/s10853-024-10529-3.

[18] J. Passaro, P. Russo, A. Bifulco, M.T. De Martino, V. Granata, B. Vitolo, G. Iannace, A. Vecchione, F. Marulo, F. Branda, Water resistant self-extinguishing low frequency soundproofing polyvinylpyrrolidone based electrospun blankets, Polymers (Basel). 11 (2019) 1205. https://doi.org/10.3390/polym11071205.

[19] C. Xu, M. Nasrollahzadeh, M. Selva, Z. Issaabadi, R. Luque, Waste-to-wealth: biowaste valorization into valuable bio (nano) materials, Chem. Soc. Rev. 48 (2019) 4791–4822. https://doi.org/10.1039/C8CS00543E.

[20] J. Glasing, P. Champagne, M.F. Cunningham, Graft modification of chitosan, cellulose and alginate using reversible deactivation radical polymerization (RDRP), Curr. Opin. Green Sustain. Chem. 2 (2016) 15–21. https://doi.org/10.1016/j.cogsc.2016.09.002.

[21] H. Vahabi, M. Jouyandeh, T. Parpaite, M.R. Saeb, S. Ramakrishna, Coffee wastes as sustainable flame retardants for polymer materials, Coatings 11 (2021) 1021. https://doi.org/10.3390/coatings11091021.

[22] I. Wani, S. Ramola, A. Garg, V. Kushvaha, Critical review of biochar applications in geoengineering infrastructure: moving beyond agricultural and environmental perspectives, Biomass Convers. Biorefinery 14 (2024) 5943–5971. https://doi.org/10.1007/s13399-021-01346-8.

[23] S. Jeffery, F.G.A. Verheijen, M. van der Velde, A.C. Bastos, A quantitative review of the effects of biochar application to soils on crop productivity using meta-analysis, Agric. Ecosyst. Environ. 144 (2011) 175–187. https://doi.org/10.1016/j.agee.2011.08.015.

[24] Y. Zhang, M. He, L. Wang, J. Yan, B. Ma, X. Zhu, Y.S. Ok, V. Mechtcherine, D.C.W. Tsang, Biochar as construction materials for achieving carbon neutrality, Biochar 4 (2022) 59. https://doi.org/10.1007/s42773-022-00182-x.

[25] Q. Zhang, H. Cai, K. Yang, W. Yi, Effect of biochar on mechanical and flame retardant properties of wood–plastic composites, Results Phys. 7 (2017) 2391–2395. https://doi.org/10.1016/j.rinp.2017.04.025.

[26] M. Bartoli, M.A. Nasir, P. Jagdale, E. Passaglia, R. Spiniello, C. Rosso, M. Giorcelli, M. Rovere, A. Tagliaferro, Influence of pyrolytic thermal history on olive pruning biochar and related epoxy composites mechanical properties, J. Compos. Mater. 54 (2020) 1863–1873.

949 https://doi.org/10.1177/0021998319888734.
950 [27] M. Giorcelli, A. Khan, N.M. Pugno, C. Rosso, A. Tagliaferro, Biochar as a cheap and
951 environmental friendly filler able to improve polymer mechanical properties, Biomass and
952 Bioenergy 120 (2019) 219–223. https://doi.org/10.1016/j.biombioe.2018.11.036.
953 [28] M. Bartoli, M. Giorcelli, C. Rosso, M. Rovere, P. Jagdale, A. Tagliaferro, Influence of
954 commercial biochar fillers on brittleness/ductility of epoxy resin composites, Appl. Sci. 9
955 (2019) 3109. https://doi.org/10.3390/app9153109.
956 [29] Tiwari, A., Raj, B. Reactions and mechanisms in thermal analysis of advanced materials.
957 John Wiley & Sons, Hoboken, NJ, 2015.
958 [30] C. Das, S. Tamrakar, A. Kiziltas, X. Xie, Incorporation of biochar to improve mechanical,
959 thermal and electrical properties of polymer composites, Polymers (Basel). 13 (2021) 2663.
960 https://doi.org/10.3390/polym13162663.
961 [31] O. Das, N.K. Kim, A.L. Kalamkarov, A.K. Sarmah, D. Bhattacharyya, Biochar to the rescue:
962 Balancing the fire performance and mechanical properties of polypropylene composites,
963 Polym. Degrad. Stab. 144 (2017) 485–496.
964 https://doi.org/10.1016/j.polymdegradstab.2017.09.006.
965 [32] O. Das, A.K. Sarmah, D. Bhattacharyya, Biocomposites from waste derived biochars:
966 Mechanical, thermal, chemical, and morphological properties, Waste Manag. 49 (2016) 560–
967 570. https://doi.org/10.1016/j.wasman.2015.12.007.
968 [33] A. Bifulco, M. Bartoli, I. Climaco, M.C. Franchino, D. Battegazzore, R.A. Mensah, O. Das,
969 H. Vahabi, G. Malucelli, A. Aronne, Coffee waste-derived biochar as a flame retardant for
970 epoxy nanocomposites, Sustain. Mater. Technol. 41 (2024) e01079.
971 https://doi.org/10.1016/j.susmat.2024.e01079.
972 [34] John, M.J. Flammability performance of biocomposites. In: Koronis, G., Silva, A. (Eds.),
973 Green Composites for Automotive Applications. Woodhead Publishing, 2019, pp. 43–58.
974 [35] M. Barbalini, M. Bartoli, A. Tagliaferro, G. Malucelli, Phytic acid and biochar: An effective
975 all bio-sourced flame retardant formulation for cotton fabrics, Polymers (Basel). 12 (2020)
976 811. https://doi.org/10.3390/polym12040811.
977 [36] L. Grande, I. Pedroarena, S.A. Korili, A. Gil, Hydrothermal liquefaction of biomass as one of
978 the most promising alternatives for the synthesis of advanced liquid biofuels: a review,
979 Materials (Basel). 14 (2021) 5286. https://doi.org/10.3390/ma14185286.
980 [37] D. Castello, T.H. Pedersen, L.A. Rosendahl, Continuous hydrothermal liquefaction of
981 biomass: A critical review, Energies 11 (2018) 3165. https://doi.org/10.3390/en11113165.
982 [38] H. Liu, I.A. Basar, A. Nzihou, C. Eskicioglu, Hydrochar derived from municipal sludge

through hydrothermal processing: A critical review on its formation, characterization, and valorization, Water Res. 199 (2021) 117186. https://doi.org/10.1016/j.watres.2021.117186.
[39] Y. Hu, S. Wang, J. Li, Q. Wang, Z. He, Y. Feng, A.E.-F. Abomohra, S. Afonaa-Mensah, C. Hui, Co-pyrolysis and co-hydrothermal liquefaction of seaweeds and rice husk: comparative study towards enhanced biofuel production, J. Anal. Appl. Pyrolysis 129 (2018) 162–170. https://doi.org/10.1016/j.jaap.2017.11.016.
[40] Z. Liu, F.-S. Zhang, J. Wu, Characterization and application of chars produced from pinewood pyrolysis and hydrothermal treatment, Fuel 89 (2010) 510–514. https://doi.org/10.1016/j.fuel.2009.08.042.
[41] Y. Ke, X. Yang, Q. Chen, J. Xue, Z. Song, Y. Zhang, S.A. Madbouly, Y. Luo, M. Li, Q. Wang, Recyclable and fluorescent epoxy polymer networks from cardanol via solvent-free epoxy-thiol chemistry, ACS Appl. Polym. Mater. 3 (2021) 3082–3092. https://doi.org/10.1021/acsapm.1c00284.
[42] V. Venezia, S. Matta, S. Lehner, G. Vitiello, A. Costantini, S. Gaan, G. Malucelli, F. Branda, G. Luciani, A. Bifulco, Detailed Thermal, Fire, and Mechanical Study of Silicon-Modified Epoxy Resin Containing Humic Acid and Other Additives, ACS Appl. Polym. Mater. 3 (2021) 5969–5981. https://doi.org/10.1021/acsapm.1c01240.
[43] F. Di Lauro, M. Balsamo, R. Solimene, M.L. Alfieri, P. Manini, R. Migliaccio, P. Salatino, F. Montagnaro, Characterization of biocrude produced by hydrothermal liquefaction of municipal sewage sludge in a 500 mL batch reactor, Ind. Eng. Chem. Res. 63 (2024) 955–967. https://doi.org/10.1021/acs.iecr.3c03058.
[44] M. Balsamo, B. Hejazi, F. Di Lauro, G. Marotta, R. Solimene, P. Salatino, F. Montagnaro, Kinetic modelling and elemental balances applied to the hydrothermal liquefaction of sewage sludge, Chem. Eng. J. 505 (2025) 158767. https://doi.org/10.1016/j.cej.2024.158767.
[45] M. Balsamo, F. Di Lauro, M.L. Alfieri, P. Manini, P. Salatino, F. Montagnaro, R. Solimene, Unravelling the role of biochemical compounds within the hydrothermal liquefaction process of real sludge mixtures, Sustainability 16 (2024) 1770. https://doi.org/10.3390/su16051770.
[46] J. Passaro, A. Bifulco, E. Calabrese, C. Imparato, M. Raimondo, R. Pantani, A. Aronne, L. Guadagno, Hybrid Hemp Particles as Functional Fillers for the Manufacturing of Hydrophobic and Anti-icing Epoxy Composite Coatings, ACS Omega 8 (2023) 23596–23606. https://doi.org/10.1021/acsomega.3c01415.
[47] D.K. Owens, Some thermodynamic aspects of polymer adhesion, J. Appl. Polym. Sci. 14 (1970) 1725–1730. https://doi.org/10.1002/app.1970.070140706.
[48] Sonnier, R., Taguet, A., Ferry, L., Lopez-Cuesta, J.-M. Towards bio-based flame retardant

polymers, 1st ed., Springer, Cham, Switzerland, 2018.
[49] B. Liu, H. Zhao, Y. Wang, Advanced flame-retardant methods for polymeric materials, Adv. Mater. 34 (2022) 2107905. https://doi.org/10.1002/adma.202107905.
[50] Y.-J. Kwon, J.-B. Park, Y.-P. Jeon, J.-Y. Hong, H.-S. Park, J.-U. Lee, A Review of Polymer Composites Based on Carbon Fillers for Thermal Management Applications: Design, Preparation, and Properties, Polymers (Basel). 13 (2021) 1312. https://doi.org/10.3390/polym13081312.
[51] I. Bejenari, R. Dinu, S. Montes, I. Volf, A. Mija, Hydrothermal Carbon as Reactive Fillers to Produce Sustainable Biocomposites with Aromatic Bio-Based Epoxy Resins, Polymers (Basel). 13 (2021) 240. https://doi.org/10.3390/polym13020240.
[52] G. Liu, H. Shi, C.K. Kundu, Z. Li, X. Li, Z. Zhang, Preparation of novel biomass humate flame retardants and their flame retardancy in epoxy resin, J. Appl. Polym. Sci. 137 (2020) 49601. https://doi.org/10.1002/app.49601.
[53] H. Yan, C. Lu, D. Jing, X. Hou, Chemical degradation of amine-cured DGEBA epoxy resin in supercritical 1-propanol for recycling carbon fiber from composites, Chinese J. Polym. Sci. 32 (2014) 1550–1563. https://doi.org/10.1007/s10118-014-1519-5.
[54] J. Passaro, C. Imparato, D. Parida, A. Bifulco, F. Branda, A. Aronne, Electrospinning of PVP-based ternary composites containing SiO2 nanoparticles and hybrid TiO2 microparticles with adsorbed superoxide radicals, Compos. Part B Eng. 238 (2022) 109874. https://doi.org/10.1016/j.compositesb.2022.109874.
[55] V.S. Smitha, P.M.A. Azeez, K.G. Warrier, B.N. Nair, U.N.S. Hareesh, Transparent and Hydrophobic MTMS/GPTMS Hybrid Aerogel Monoliths and Coatings by Sol-Gel Method: A Viable Remedy for Oil-Spill Cleanup, ChemistrySelect 3 (2018) 2989–2997. https://doi.org/10.1002/slct.201702967.
[56] Horrocks, A.R., Price, D., Price, D. Fire retardant materials. Woodhead Publishing, 2001.
[57] K. Koch, B. Bhushan, Y.C. Jung, W. Barthlott, Fabrication of artificial Lotus leaves and significance of hierarchical structure for superhydrophobicity and low adhesion, Soft Matter 5 (2009) 1386–1393. https://doi.org/10.1039/B818940D.
[58] X.-F. Zhang, X.-D. Li, N. Wang, Y.-J. Liu, F. Tian, C.-X. Wang, Robust superhydrophobic SiO2/epoxy composite coating prepared by one-step spraying method for corrosion protection of aluminum alloy: Experimental and theoretical studies, Mater. Des. 228 (2023) 111833. https://doi.org/10.1016/j.matdes.2023.111833.
[59] V.K. Ponnusamy, S. Nagappan, R.R. Bhosale, C.-H. Lay, D.D. Nguyen, A. Pugazhendhi, S.W. Chang, G. Kumar, Review on sustainable production of biochar through hydrothermal

liquefaction: Physico-chemical properties and applications, Bioresour. Technol. 310 (2020) 123414. https://doi.org/10.1016/j.biortech.2020.123414.

[60] P. Zheng, H. Zhao, J. Li, Q. Liu, X. Yang, Y. Zhou, Enhance the fire safety of epoxy resin using ammonium polyphosphate flame retardant with the sandwich structure containing catalytic carbon formation function, J. Appl. Polym. Sci. 141 (2024) e55587. https://doi.org/10.1002/app.55587.

[61] B.K. Kandola, F. Magnoni, J.R. Ebdon, Flame retardants for epoxy resins: Application-related challenges and solutions, J. Vinyl Addit. Technol. 28 (2022) 17–49. https://doi.org/10.1002/vnl.21890.

[62] L. Yi, M. Long, L. Yan, X. Tang, J. Liao, A facile strategy to construct multifunctional microencapsulated urea ammonium polyphosphate for epoxy resins towards satisfied fire safety, thermal stability and compatibility, J. Appl. Polym. Sci. 140 (2023) e53675. https://doi.org/10.1002/app.53675.

[63] A.M. Gaifutdinov, K.A. Andrianova, L.M. Amirova, V.A. Milyukov, A.A. Zagidullin, R.R. Amirov, Low-flammability carbon fiber reinforced composites based on low-viscosity phosphorus-containing epoxy binders for transfer molding methods, Mater. Today Commun. 40 (2024) 109340. https://doi.org/10.1016/j.mtcomm.2024.109340,

[64] Z. Cheng, M. Fang, X. Chen, Y. Zhang, Y. Wang, H. Li, J. Qian, Thermal stability and flame retardancy of a cured trifunctional epoxy resin with the synergistic effects of silicon/titanium, ACS Omega 5 (2020) 4200–4212. https://doi.org/10.1021/acsomega.9b04050.

[65] A. Ishak, C. Longuet, B. Otazaghine, R. Sonnier, Synthesis of novel reactive flame retardant to improve fire resistance and mechanical properties in epoxy resin, Polym. Degrad. Stab. 228 (2024) 110925. https://doi.org/10.1016/j.polymdegradstab.2024.110925.

[66] D. Yu, J. Guo, J. Meng, T. Sun, Biofuel production by hydro-thermal liquefaction of municipal solid waste: Process characterization and optimization, Chemosphere 328 (2023) 138606. https://doi.org/10.1016/j.chemosphere.2023.138606.

[67] P. Li, L. Li, L. Ji, L. Dang, S. Lan, D. Zhu, Functionalized magnesium hydroxide with zinc borate and 3-aminopropyltriethoxysilane for enhanced flame retardant and smoke suppressant properties of epoxy resins, J. Appl. Polym. Sci. 140 (2023) e53941. https://doi.org/10.1002/app.53941.

[68] G. Camino, G. Tartaglione, A. Frache, C. Manferti, G. Costa, Thermal and combustion behaviour of layered silicate–epoxy nanocomposites, Polym. Degrad. Stab. 90 (2005) 354–362. https://doi.org/10.1016/j.polymdegradstab.2005.02.022.

[69] J. Zhong, E. Wang, Y. Sun, N. Yin, S. Tian, W. Ying, W. Li, W. Zhang, Fabrication of

phytic acid/urea co-modified bamboo biochar and its application as green flame retardant for polylactic acid resins, Polymers (Basel). 15 (2023) 360. https://doi.org/10.3390/polym15020360.

[70] M. Wang, Z. Zhu, C. Cheng, H. Sun, J. Li, R. Jiao, A. Li, A novel conjugated microporous polymer nano hollow sphere containing N, P and Si flame retardant elements with both thermal insulation and flame retardant properties, Colloids Surfaces A Physicochem. Eng. Asp. 704 (2025) 135490. https://doi.org/10.1016/j.colsurfa.2024.135490.

[71] X. Qiu, X. Wan, Z. Wang, Z. Li, J. Li, X. Li, Z. Zhang, A simple and universal strategy for construction and application of silica-based flame-retardant nanostructure, Compos. Part B Eng. 238 (2022) 109887. https://doi.org/10.1016/j.compositesb.2022.109887.

[72] Y. Wang, Y. Zhang, L. Ma, H. Ge, J. Gao, Z. Zhu, Y. Weng, Facile synthesis of phosphorus-containing benzotriazole flame retardant for enhancement of mechanical and fire properties of epoxy resins, Eur. Polym. J. 202 (2024) 112610. https://doi.org/10.1016/j.eurpolymj.2023.112610.

[73] Á. Pomázi, A. Toldy, Development of fire retardant epoxy-based gelcoats for carbon fibre reinforced epoxy resin composites, Prog. Org. Coatings 151 (2021) 106015. https://doi.org/10.1016/j.porgcoat.2020.106015.

[74] J.S. Baisch, C.L. Djadjo, É.J. Alves Nunes, L. de Oliveira Carneiro, M.V. Tres, G.L. Zabot, Promising products based on hydrothermal liquefaction of agricultural biomass: an overview, Discov. Appl. Sci. 7 (2025) 1–22. https://doi.org/10.1007/s42452-025-06898-2.

[75] S. Gaan, G. Sun, K. Hutches, M.H. Engelhard, Effect of nitrogen additives on flame retardant action of tributyl phosphate: phosphorus–nitrogen synergism, Polym. Degrad. Stab. 93 (2008) 99–108. https://doi.org/10.1016/j.polymdegradstab.2007.10.013.

[76] A. Bifulco, R. Avolio, S. Lehner, M.E. Errico, N.J. Clayden, R. Pauer, S. Gaan, G. Malucelli, A. Aronne, C. Imparato, In situ P-modified hybrid silica–epoxy nanocomposites via a green hydrolytic sol–gel route for flame-retardant applications, ACS Appl. Nano Mater. 6 (2023) 7422–7435. https://doi.org/10.1021/acsanm.3c00590.

[77] Y. Tan, Z.-B. Shao, L.-X. Yu, Y.-J. Xu, W.-H. Rao, L. Chen, Y.-Z. Wang, Polyethyleneimine modified ammonium polyphosphate toward polyamine-hardener for epoxy resin: Thermal stability, flame retardance and smoke suppression, Polym. Degrad. Stab. 131 (2016) 62–70. https://doi.org/10.1016/j.polymdegradstab.2016.07.004.

[78] M.-O. Augé, D. Roncucci, F. Bonnet, S. Bourbigot, S. Gaan, G. Fontaine, Improving poly (lactic acid) fire performances via blending with benzoxazine, Polym. Degrad. Stab. 230 (2024) 111032. https://doi.org/10.1016/j.polymdegradstab.2024.111032.

[79] J. Fang, R. Zuo, P. He, Y. Quan, Q. Chen, The effect of urea bond on structure and properties of toughened epoxy resins, J. Appl. Polym. Sci. 118 (2010) 2195–2201. https://doi.org/10.1002/app.32594.

[80] R. Rajan, E. Rainosalo, S.K. Ramamoorthy, S.P. Thomas, J. Zavašnik, J. Vuorinen, M. Skrifvars, Mechanical, thermal, and burning properties of viscose fabric composites: Influence of epoxy resin modification, J. Appl. Polym. Sci. 135 (2018) 46673. https://doi.org/10.1002/app.46673.

[81] X. Qin, Y. Tian, H. Zhao, J. Wang, S. Zhan, J. Qu, L. Zhang, J. Liu, Toward Reprocessable High-Performance Elastomer: Self-Assembly, Dynamic Covalent Chemistry, and Tailorable Properties, Adv. Mater. 37 (2025) e15432. https://doi.org/10.1002/adma.202515432.

[82] M.K. Umboh, T. Adachi, K. Oishi, M. Higuchi, Z. Major, Mechanical properties of nano-silica particulate-reinforced epoxy composites considered in terms of crosslinking effect in matrix resins, J. Mater. Sci. 48 (2013) 5148–5156. https://doi.org/10.1007/s10853-013-7300-2.

[83] A.M. Goula, K.G. Adamopoulos, Effect of maltodextrin addition during spray drying of tomato pulp in dehumidified air: I. Drying kinetics and product recovery, Dry. Technol. 26 (2008) 714–725. https://doi.org/10.1080/07373930802046369.

[84] J.S. George, P. Vijayan P, M. Poncot, H. Vahabi, H.J. Maria, S. Thomas, Insights into the synergistic effect of graphene oxide/silica hybrid nanofiller for advancing the properties of epoxy resin, ACS Appl. Polym. Mater. 6 (2024) 5932–5944. https://doi.org/10.1021/acsapm.4c00601.

[85] L. Zhu, M. Li, S. Zhao, S. Bao, F. Chen, Y. Shangguan, Q. Wu, Q. Zheng, Ultra-high impact PPR composites at low-temperature through enhanced preferential loading of nanoparticles at polymeric interface induced by properly vulcanized rubber dispersed phase, Compos. Sci. Technol. 227 (2022) 109593. https://doi.org/10.1016/j.compscitech.2022.109593.

[86] H. Gan, S.M. Seraji, R.B. Senanayake, S.R. Swan, J. Zhang, R.J. Varley, A DOPO modified cyclosiloxane reactive diluent as an effective flame retardant for a high-performance epoxy network, Polymer (Guildf). 309 (2024) 127427. https://doi.org/10.1016/j.polymer.2024.127427.

[87] J. Zhang, Z. Zhang, R. Huang, L. Tan, Advances in Toughening Modification Methods for Epoxy Resins: A Comprehensive Review, Polymers (Basel). 17 (2025) 1288. https://doi.org/10.3390/polym17091288.

[88] N. Sathiya Narayanan, D. Sai Venkat Mohan, J. Abhinay, T. Dinesh, V. Satya Sai Surya Teja, R. Praneeth, Effects on microhardness, tensile strength, deflection, and drop weight

impact resistance with the addition of hybrid filler materials for enhancing GFRP composites, Sci. Rep. 14 (2024) 27524. https://doi.org/10.1038/s41598-024-76094-6.

Graphical abstract